Seabed Shear Stress Estimates at the Cohasset and Hibernia Oil Production Sites

C. Anderson

Ocean Sciences Division
Maritimes Region
Fisheries and Oceans Canada

Bedford Institute of Oceanography
P.O. Box 1006
Dartmouth, Nova Scotia
Canada B2Y 4A2

2001

Canadian Technical Report of Hydrography and Ocean Sciences 216

Fisheries and Oceans Canada | Pêches et Océans Canada

Canada

Canadian Technical Report of
Hydrography and Ocean Sciences 216

2001

Seabed Shear Stress Estimates at the Cohasset and Hibernia Oil Production Sites

by

Carl Anderson[1]

Ocean Sciences Division
Maritimes Region
Department of Fisheries and Oceans
Bedford Institute of Oceanography
P.O. Box 1006
Dartmouth, Nova Scotia
Canada B2Y 4A2

[1] Challenger Oceanography, 25 Lawnsdale Drive, Dartmouth, Nova Scotia, Canada, B3A 2N1

©Public Works and Government Services 2001
Cat. No. Fs 97-18/216E ISSN 0711-6764

Correct citation for this publication:

Anderson, Carl. 2001. Seabed shear stress estimates at the Cohasset and Hibernia oil production sites. Can. Tech. Rep. Hydrogr. Ocean Sci. 216: viii + 54 pp.

102-00149/

Seabed Shear Stress Estimates at the Cohasset and Hibernia Oil Production Sites

Contents

1 Introduction 1
2 Observations 1
2.1 Currents 1
2.2 Waves 2
2.3 Merging the data 4
3 Sensitivity analysis 4
3.1 Parameter ranges 4
3.2 Results 4
3.3 Conclusions 4
4 Site-specific Computations 5
4.1 Physical parameters 5
4.2 Bed shear velocity 5
4.3 Sediment transport 5
4.4 Critical shear velocities 6
5 Results 6
5.1 Seabed shear velocities 6
5.2 Sediment transport 6
6 Discussion 7
6.1 Currents 7
6.2 Waves 7
6.3 Shear velocities 8
6.4 Sediment transport 8
7 Conclusions 8
8 Acknowledgements 9
9 References 10

Tables

Table 1. Summary of Cohasset and Hibernia current meter deployments, 1993-2000. 11

Table 2. Details of Cohasset ADCP data coverage, 1993-1996. All times are UTC. 11

Table 3. Details of Hibernia current meter deployments, 1998-2000. All times are UTC 11

Table 4. Statistics of hourly ADCP near-seabed current measurements at Cohasset, in the years 1993-1996. 12

Table 5. Statistics of the ADCP near-seabed current measurements at Cohasset, for the hours in which there were data in all of the years 1993-1996 (13 hrs 28 September to 22 hrs 22 November, one day later in 1996, a leap year). 12

Table 6. Statistics of hourly near-seabed current measurements at the Hibernia SE and NE sites, for the period of the measurements at the SE site (1700 hrs 19 Feb to 1600 hrs 5 June). 13

Table 7. Statistics of the combined hourly current time series at Hibernia in the years 1998-2000. 13

Table 8. Statistics of 3-hourly Cohasset swell wave observations concurrent with ADCP measurements and with swell height greater than zero ($H > 0$), in the years 1993-1996. 14

Table 9. Statistics of 3-hourly Hibernia GBS swell wave observations concurrent with nearby current measurements and with swell height greater than zero ($H > 0$), in the years 1998-2000. 14

Table 10. Critical shear velocities for medium sand with grain diameter GD = 0.00025 m. 15

Table 11. Statistics of estimated seabed shear velocity u_{*cws} at Cohasset, in the years 1993-1996. 15

Table 12. Statistics of estimated seabed shear velocity u_{*cws} at Hibernia, in the years 1998-2000. 15

Table 13. Statistics of predicted volumetric rate of sediment transport at Cohasset, in the years 1993-1996. 16

Table 14. Statistics of predicted volumetric rate of sediment transport at Hibernia, in the years 1998-2000. 16

Figures

Figure 1. Hourly time series of swell height *H*, period *T*, and near-seabed current *U(z)*, at Cohasset, 1993. 17

Figure 2. Hourly time series of swell height *H*, period *T*, and near-seabed current *U(z)*, at Cohasset, 1995. 18

Figure 3. Hourly time series of swell height *H*, period *T*, and near-seabed current *U(z)*, at Cohasset, 1996. 19

Figure 4. Hourly time series of swell height *H*, period *T*, and near-seabed current *U(z)*, at Hibernia, 1998. 20

Figure 5. Hourly time series of swell height *H*, period *T*, and near-seabed current *U(z)*, at Hibernia, 1999. 21

Figure 6. Hourly time series of swell height *H*, period *T*, and near-seabed current *U(z)*, at Hibernia, 2000. 22

Figure 7. Histograms of hourly swell height *H*, period *T*, current magnitude *U(z)*, and skin-friction combined shear velocity u_{*cws} at Cohasset, 1993. 23

Figure 8. Histograms of hourly swell height *H*, period *T*, current magnitude *U(z)*, and skin-friction combined shear velocity u_{*cws} at Cohasset, 1995. 24

Figure 9. Histograms of hourly swell height *H*, period *T*, current magnitude *U(z)*, and skin-friction combined shear velocity u_{*cws} at Cohasset, 1996. 25

Figure 10. Histograms of hourly swell height *H*, period *T*, current magnitude *U(z)*, and skin-friction combined shear velocity u_{*cws} at Hibernia, 1998. 26

Figure 11. Histograms of hourly swell height *H*, period *T*, current magnitude *U(z)*, and skin-friction combined shear velocity u_{*cws} at Hibernia, 1999. 27

Figure 12. Histograms of hourly swell height *H*, period *T*, current magnitude *U(z)*, and skin-friction combined shear velocity u_{*cws} at Hibernia, 2000. 28

Figure 13. Polar plots of hourly near-seabed current *U(z)* magnitude versus current direction (toward), and hourly swell height *H* versus swell direction (from) at Cohasset, 1993. 29

Figure 14. Polar plots of hourly near-seabed current *U(z)* magnitude versus current direction (toward), and hourly swell height *H* versus swell direction (from) at Cohasset, 1995. 30

Figure 15. Polar plots of hourly near-seabed current *U(z)* magnitude versus current direction (toward), and hourly swell height *H* versus swell direction (from) at Cohasset, 1996. 31

Figure 16. Polar plots of hourly near-seabed current *U(z)* magnitude versus current direction (toward), and hourly swell height *H* versus swell direction (from) at Hibernia, 1998. 32

Figure 17. Polar plots of hourly near-seabed current *U(z)* magnitude versus current direction (toward), and hourly swell height *H* versus swell direction (from) at Hibernia, 1999. 33

Figure 18. Polar plots of hourly near-seabed current *U(z)* magnitude versus current direction (toward), and hourly swell height *H* versus swell direction (from) at Hibernia, 2000. 34

Figure 19. Wave types observed at Cohasset, 1993. 35

Figure 20. Wave types observed at Cohasset, 1995. 36

Figure 21. Wave types observed at Cohasset, 1996. 37

Figure 22. Wave types observed at Hibernia, 1998 38

Figure 23. Wave types observed at Hibernia, 1999 39

Figure 24. Wave types observed at Hibernia, 2000 40

Figure 25. Seabed shear velocity u_{*cws} versus wave height for water depths from 10 to 60 m and sediment grain diameter 32μ (0. 032 mm). 41

Figure 26 Seabed shear velocity u_{*cws} versus wave height for water depths from 10 to 60 m and sediment grain diameter 63μ (0. 063 mm). 42

Figure 27 Seabed shear velocity u_{*cws} versus wave height for water depths from 10 to 60 m and sediment grain diameter 125μ (0. 125 mm). 43

Figure 28 Seabed shear velocity u_{*cws} versus wave height for water depths from 10 to 60 m and sediment grain diameter 250μ (0. 250 mm). 44

Figure 29. Seabed shear velocity u_{*cws} versus wave height for water depths from 10 to 60 m and sediment grain diameter 500μ (0. 500 mm). 45

Figure 30 Seabed shear velocity u_{*cws} versus wave height for water depths from 10 to 60 m and sediment grain diameter 1000μ (0. 100 mm). 46

Figure 31. Surficial Geology of the Hibernia area, Northeast Grand Banks of Newfoundland. From Barrie *et al*, 1984. 47

Figure 32. Surficial sediment grain size distribution, Hibernia area, Northeast Grand Banks of Newfoundland. From Barrie *et al*, 1984. 48

Figure 33. Hourly time series of swell height *H*, near-seabed current *U(z)*, skin-friction combined shear velocity u_{*cws}, and volumetric rate of sediment transport magnitude at Cohasset, 1993. 49

Figure 34. Hourly time series of swell height *H*, near-seabed current *U(z)*, skin-friction combined shear velocity u_{*cws}, and volumetric rate of sediment transport magnitude at Cohasset, 1995. 50

Figure 35. Hourly time series of swell height *H*, near-seabed current *U(z)*, skin-friction combined shear velocity u_{*cws}, and volumetric rate of sediment transport magnitude at Cohasset, 1996. 51

Figure 36. Hourly time series of swell height H, near-seabed current $U(z)$, skin-friction combined shear velocity u_{*cws}, and volumetric rate of sediment transport magnitude at Hibernia, 1998.....52

Figure 37. Hourly time series of swell height H, near-seabed current $U(z)$, skin-friction combined shear velocity u_{*cws}, and volumetric rate of sediment transport magnitude at Hibernia, 1999.....53

Figure 38. Hourly time series of swell height H, near-seabed current $U(z)$, skin-friction combined shear velocity u_{*cws}, and volumetric rate of sediment transport magnitude at Hibernia, 2000.....54

Seabed Shear Stress Estimates at the Cohasset and Hibernia Oil Production Sites

Abstract

Anderson, Carl. 2001. Seabed shear stress estimates at the Cohasset and Hibernia oil production sites. Can. Tech. Rep. Hydrogr. Ocean Sci. 216: viii + 54 pp.

A one-dimensional sediment transport model was used to evaluate seabed shear stress and volumetric rate of sediment transport at two East Coast Canadian offshore oil production sites– Cohasset, on Sable Island Bank, and Hibernia, on the Grand Banks of Newfoundland. Input to the model were (1) near-seabed current measurements and (2) surface wave (swell) observations in 1993 and 1995-1996 (Cohasset), and 1998-2000 (Hibernia). Surficial sediment grain size and density were assigned realistic site-specific values. Results are reported as time series of stress velocity and volumetric rate of sediment transport. Statistics and histograms of the input and output variables are also reported.

A sensitivity analysis was also performed to examine the dependence of seabed shear stress on current, wave height, and surficial sediment grain size.

Résumé

Anderson, Carl. 2001. Seabed shear stress estimates at the Cohasset and Hibernia oil production sites. Can. Tech. Rep. Hydrogr. Ocean Sci. 216: viii + 54 pp.

Un modèle unidimensionnel de transport de sédiments a servi à évaluer la contrainte de cisaillement du plancher océanique et le taux volumétrique du transport de sédiments dans deux sites de production d'hydrocarbure extracôtier, soit le site de Cohasset, sur le banc de l'île de Sable et le site d'Hibernia, sur les Grands Bancs de Terre-Neuve. Les entrées du modèle se composaient 1) de mesures du courant près du plancher océanique et 2) d'observations des ondes de surface (houle) réalisées en 1993, en 1995 et en 1996 (Cohasset) ainsi que de 1998 à 2000 (Hibernia). On a attribué à la granulométrie et à la densité des sédiments superficiels des valeurs réalistes particulières au site. Les résultats sont présentés sous forme de séries chronologiques de la vitesse de la contrainte et du taux volumétrique du transport des sédiments. On fournit aussi des statistiques et des histogrammes des variables d'entrée et de sortie.

Une analyse de sensibilité a également été effectuée pour examiner la relation de dépendance entre la contrainte de cisaillement du plancher océanique et le courant, le creux de vague et la granulométrie des sédiments superficiels.

Seabed Shear Stress Estimates at the Cohasset and Hibernia Oil Production Sites

1 Introduction

Offshore petroleum operators routinely measure ocean currents near offshore rigs, and make weather and sea state observations as part of their Physical Environment Programs. Additional current measurements have been made at the Hibernia production site on the Grand Banks as part of PERD (Program for Energy Research and Development) studies of currents and the fate of drilling wastes. Near-seabed current measurements and surface wave data gathered as part of these programs were used to estimate seabed shear stress at two oil production sites on the eastern Canadian continental shelf- the Cohasset site on Sable Island Bank (Anderson, 1998), and the Hibernia site on the Grand Banks of Newfoundland (Anderson, 2001). Computations in both cases were made using the one-dimensional sediment transport model SEDTRANS96 (Li and Amos, 1997).

This report brings together the results of the Cohasset and Hibernia stress computations. Included is a sensitivity study that examines the sensitivity of the stress estimates to varying surface wave height and surficial sediment grain size for various water depths and near-seabed currents.

2 Observations

The observations used in the studies were made at the Cohasset oil production site on Sable Island Bank (43°51' N, 60°38' W, nominal water depth $D = 43$ m) in 1993, 1995, and 1996, and near the Hibernia oil production site (Gravity Based Structure, or GBS) on the Newfoundland Grand Banks (46° 45.0' N, 48° 46.9' W, $D \approx 80$ m) in 1998-2000 (Table 1).

2.1 Currents

Cohasset

Currents were measured at the Cohasset site by a seabed-mounted, upward-looking Acoustic Doppler Current Meter (ADCP). The ADCP field deployments and data processing are described in data reports by Coastal Ocean Associates (COA, 1997, 1998), which also present plots and tidal analysis of the current profiles. COA (1999) describes quality problems that were encountered in processing the ADCP data, and discusses measures taken to resolve these problems. The current meter data were provided by the Department of Fisheries and Oceans (DFO), and consisted of hourly observations of the vector velocity (u,v) in approximately 1 m-thick velocity bins from near the seabed to the surface.

Time series of the Cohasset near-seabed current magnitude are plotted for 1993, 1995, and 1996 in Figure 1 - Figure 3. Histograms of current speed are shown in Figure 7 - Figure 9. The directional distribution and magnitude of the near-seabed current are shown in Figure 13 - Figure 15, in which current speed is plotted versus current direction for each year of the study. Table 4 summarises the statistics of the current measurements for 1993 and 1995-96. There were

no ADCP observations at the Cohasset site in 1994. Current statistics are presented in Table 5 for the hours of the year during which ADCP data were available in all three years (1329 hours, 13 hrs 28 September to 22 hrs 22 November, one day later in 1996, a leap year).

Hibernia

Current was measured at two sites within 4 km of the Hibernia GBS, as part of the Offshore Environmental Factors and Impacts programs of PERD. The data used here were obtained from Aanderaa current meters moored at 3 m above the seabed (see Geshelin *et al* 2001 for further information).

The Hibernia current meter data were provided by DFO as time series of the near-seabed current speed and direction ($U(z), \theta$) at a height z = 3 m above the seabed. Details of the deployments are given in Table 3. Current measurements were recorded at 0.5-hr intervals (0 and 30 minutes past the hour UT) at a site approximately 3.8 km southeast of the GBS (SE site, Deployment I). These data were sub-sampled at 0 minutes past the hour UT for the purposes of this study.

Measurements at 1-hr intervals (0 minutes past the hour UT) came from another site approximately 1.7 km northeast of the Hibernia GBS (NE site, Deployments II, III, IV). The current meter mooring at the NE site was recovered and re-deployed on two occasions, between deployments II and III, and III and IV. In the data received from DFO, the data gaps resulting from the recoveries and redeployments (3 and 5hrs, respectively) had been filled by linear interpolation of $U(z)$ and θ (Yuri Geshelin, DFO, personal communication).

To assess whether the currents measured at both sites were representative of the current regime around the Hibernia GBS, the time-domain statistics of the 1-hr current time series at the SE and NE sites were compared (Table 6) for the period of the shorter (2,544-hr) current meter deployment at the SE site (1700 hrs 19 Feb to 1600 hrs 5 June). The table presents the maximum current magnitude U_{max}, vector mean current speed and direction ($U(z)_{mean}$, θ_{mean}), and the orientation $\theta_{principal}$ of the principal axes of the current. The root-mean-square values of the variable component of the current resolved on the major and minor principal axes, v'_{RMS} and u'_{RMS}, are also shown.

The full hourly time series of Hibernia near-seabed current magnitude and direction are plotted for the years 1998, 1999, and 2000 in Figure 4 - Figure 6. Statistics for the current time series are presented in Table 7 by year.

Histograms of current speed are shown for Hibernia in Figure 10 - Figure 12. The directional distribution of the near-seabed current is shown in Figure 16 - Figure 18, where current speed is plotted versus current direction for each year of the study.

2.2 Waves

Cohasset

Meteorological observations were made by weather observers stationed on the Cohasset platform and the Hibernia GBS on the eight (8) semi-synoptic hours (00, 03, 06, 09, 12, 15, 18, 21 hrs UT), generally in accordance with the Manual of Marine Weather Observing (MANMAR, Environment Canada, 1982). The wave observations relevant to these analyses are the estimates

of primary swell height, period, and direction. In accordance with MANMAR, swell height H is recorded to the nearest 0.5 m, period T to the nearest whole second, and direction θ, to the nearest 10°.

Monthly MANMAR data from Cohasset were provided by DFO (obtained from Seimac, Ltd.)for 1993-1996. The monthly files were first checked for missing and extra records. Duplicate records were eliminated, and the few missing records were filled in by duplicating adjacent records. The twelve monthly data files for each year were then combined into 1-year direct-access files for merging with the current meter observations.

Time series of Cohasset swell height H and period T are plotted for 1993 and 1995-1996 in Figure 1 - Figure 3. Swell observations are shown only for the hours for which ADCP measurements were available. Histograms of swell height and period are shown in Figure 7 - Figure 9. The histogram for wave period T does not include the (undefined) swell period for reported calm seas ($H = 0$).

The wave types corresponding to the swell observations at Cohasset in 1993 and 1995-1996 are plotted in Figure 19 - Figure 21. The observations are plotted as wave height normalised by depth (H/D) versus depth divided by the Airy wavelength (D/L). The plots show the wave types included in the data sets, but not their frequencies of occurrence. See Komar (1976) for an explanation of the wave type regions shown on this plot.

The statistics of the MANMAR wave observations are presented for Cohasset in Table 8. Wave height statistics are for those hours in each year for which ADCP measurements were available; wave period statistics do not include those hours when calm seas were reported ($H = 0$).

Hibernia

Monthly MANMAR data for Hibernia were provided by AMEC Earth and Environmental, St. John's, NF, who co-ordinate the Hibernia Physical Environment Program. The monthly MANMAR files were first checked for extraneous, missing, or faulty records. Extraneous records were eliminated, and the time series was padded to correct for missing records in seven (7) places. Wave observations in the seven padding records was taken from adjacent records. Two (2) faulty timestamps were found and corrected. The twelve monthly data files for each year were then concatenated into 1-year-long files with the original sampling interval of 3 hours.

The statistics of the Hibernia 3-hourly MANMAR wave observations are presented in Table 9. Statistics are for only those hours in each year with concurrent current measurements, and for which the swell height was greater than zero ($H > 0$).

Hourly time series of Hibernia swell height H and period T are plotted for 1998, 1999 and 2000 in Figure 4 - Figure 6. Histograms of swell height and period are shown in Figure 10 - Figure 12. The histograms for T do not include wave observations when swell height was zero ($H = 0$, T not defined).

The wave types corresponding to the hourly Hibernia swell data for 1998, 1999 and 2000 are plotted in Figure 22 - Figure 24.

2.3 Merging the data

Hourly wave time series for Cohasset were created from the 3-hourly synoptic wave observations by assigning the closest semi-synoptic wave observation to the non-synoptic hours. The resulting hourly wave time series were aligned and merged with the hourly ADCP current time series.

The Hibernia 30-minute current time series from the SE site were sub-sampled at an interval of one hour, in common with the NE current meter data, and the 3-hourly swell observations were interpolated to a 1-hour sampling interval. The 1-hour data were then aligned and merged to form an input data set for each of the years of the study.

3 Sensitivity analysis

A sensitivity study was conducted to examine the sensitivity of the *skin-friction combined wave-current shear velocity u*cw*, as calculated by SEDTRANS96, to wave height H and surficial sediment grain size *GD* for a range of near-seabed currents *U(z)* and water depths *D*.

3.1 Parameter ranges

The analysis was conducted by running SEDTRANS96 with constant wave period $T = 8$ seconds, and varying the other parameters over the following ranges: sediment grain size *GD* from 32 to 1000 μ (0.032 to 1.000 mm), depth $D = 10$ to 60 m, and near-seabed current $U(z) = 0.10$ m/s and 0.30 m/s at $z = 2.5$ m.

3.2 Results

The results of the sensitivity study are presented as constant-grain-size plots in which the seabed shear velocity u_{*cw} is plotted as a function of wave height for currents $U(z) = 0.10$ and 0.30 m/s and depths $D = 10$, 20, 30, 40, 50, and 60 m. Figure 25 - Figure 30 are drawn for grain diameters *GD* of 32, 63, 125, 400, 500, and 1000μ. Also shown on each plot are the critical shear stress velocities u_{*crb} and u_{*crs} for the initiation of bedload and suspended transport, respectively.

3.3 Conclusions

The results of the sensitivity analysis are useful in identifying the relative importance of various parameters to seabed stress, and in determining under what circumstances the seabed shear stress can be estimated with reasonable accuracy *in the absence* of surface wave measurements, *i.e.*, using near-seabed current measurements alone.

The results show that in shallow water, waves have a stronger influence on bed shear velocity than in deep water, as expected. Therefore, bed shear velocity cannot be estimated from seabed current measurements alone in shallow water; wave measurements are also required. In deep water, except in extreme storm conditions, a reasonable estimate of u_{*cw} may be obtained from seabed current measurements alone. The dividing line between deep to shallow water, for 8-second period waves appears to be 60 m.

The analysis also indicates that, for a given water depth and near bed current, bed shear velocity varies nearly linearly as the *logarithm* of the grain diameter. Therefore, either halving or doubling the grain diameter has the same relative effect on the calculated bed shear. The plots also show that everywhere in the range of parameters used, halving or doubling the grain diameter changes the estimated bed shear by less than ± 10%.

4 Site-specific Computations

Seabed shear stress and the volumetric rate of sediment transport were estimated by applying SEDTRANS96 to the merged hourly time series of near-seabed current and surface swell. The analysis program required several physical parameters to be established, as described in the next section. The output variables are described below.

4.1 Physical parameters

The Cohasset production platform was situated on Sable Island Bank, where the surficial sediment is more than 90% sand (Amos, 1990). Amos and Nadeau (1988) present a grain size distribution map of Sable Island Bank that indicates a grain size of 250μ at the Cohasset site. In the seabed stress and sediment transport computations reported here, the grain size parameter *GD* was therefore set at 0.00025 m. Sediment density was taken to be 2650 kg/m^3, and the density of sea water ρ_w, 1025 kg/m^3.

The Hibernia GBS is situated on a sand ridge designated as Unit E, Sand Ridge Field in Figure 31. In the figure, the Hibernia GBS is located at the site labelled P-15 wellsite. The SE and NE current meter sites (not plotted in the figure) are within 3.8 km southeast and northeast of P-15, respectively, on the eastern flank of the sand ridge. The surficial sediment was taken to be a medium sand (Barrie *et al*, 1984, Figure 32), with characteristic grain diameter of 0.25 mm, or 250μ (T. Milligan, BIO, personal communication). At Hibernia, therefore, the physical parameters *GD*, ρ_s, and ρ_w were assigned the same values as at Cohasset.

4.2 Bed shear velocity

The seabed shear velocities were calculated by SEDTRANS96 (Li and Amos, 1997). SEDTRANS96 estimates the combined wave-current seabed shear stress τ_{cws} using the method of Grant and Madsen (1979, 1982, 1986). The seabed shear velocity reported here is shear velocity relevant to the initiation of sediment suspension: the *skin-friction combined wave-current shear velocity* $u_{*cws} = \sqrt{\tau_{cws}/\rho_w}$, where ρ_w is the density of seawater (1025 kg/m^3). (See Li and Amos (1997), pages 22 and 80.)

4.3 Sediment transport

Sediment transport is initiated when the seabed shear velocity exceeds the threshold critical shear velocity. Once initiated, the rate of sediment transport for a given seabed shear stress depends on

the magnitude of the ambient current, and the properties of the surface wave. In the presence of waves, SEDTRANS96 predicts the magnitude and direction of the sediment transport by integrating the effect of the seabed stress over one wave period. The sediment transport algorithm used in this study is that of Bagnold (1963), in which there is no distinction between near-seabed current direction and the direction of sediment transport.

4.4 Critical shear velocities

Different modes of transport predominate when the shear velocities increase beyond the initiation threshold. Table 10 gives the critical shear velocities for various transport modes for the medium sand at the Hibernia site (grain diameter GD = 0.00025 m). The settling velocity for this sand is 0.0284 m/s.

5 Results

The output of SEDTRANS96 were (1) estimated skin-friction combined wave-current shear velocity u_{*cws} and (2) the estimated volumetric rate of sediment transport. Time series plots of these variables are presented here with summary statistics for each year of the study.

5.1 Seabed shear velocities

The calculated time series of wave-current bed shear velocity u_{*cws} are plotted in Figure 33 - Figure 35 for Cohasset, and in Figure 36 - Figure 38 for Hibernia, for the hours for which current measurements were available. Hourly time series of wave height H and near-seabed current $U(z)$ are repeated in these figures from Figure 1 - Figure 3 (Cohasset) and Figure 4 - Figure 6 (Hibernia). Histograms of u_{*cws} are plotted in Figure 7 - Figure 9 for Cohasset, and Figure 10 - Figure 12 for Hibernia. The statistics of the bed shear velocity u_{*cws} are shown for Cohasset in Table 11, and for Hibernia, in Table 12.

5.2 Sediment transport

For the specified grain diameter (0.00025 m) and uniform flat seabed, SEDTRANS96 predicts the threshold for the initiation of bedload transport u_{*crb} = 0.0137 m/s, and the threshold for the initiation of suspended load transport u_{*crs} = 0.0226 m/s (Table 10). Therefore, at both sites, whenever the skin-friction combined shear velocity u_{*cws} was less than u_{*crb} = 0.0137 m/s, no sediment transport occurred. When the critical shear velocity was exceeded, SEDTRANS96 estimated the magnitude of the volumetric rate of sediment transport V, defined as the sediment volume flux per unit seabed width (normal to the transport direction) per unit time ($m^3/m/s$).

The estimated sediment volume transports are potted in Figure 33 - Figure 35 for the Cohasset site, and in Figure 36 - Figure 38 for Hibernia. The statistics of the estimated volumetric rates of sediment transport (magnitude and direction) are shown in Table 13 for Cohasset, and Table 14 for Hibernia.

6 Discussion

6.1 Currents

The polar plots of near-seabed current 2.7 m above the seabed at Cohasset (Figure 13 -Figure 15) strongly suggest that the flow field measured by the ADCP was distorted in a consistent manner from year to year. Similar polar plots of the current farther from the seabed (not shown; see Anderson 1998) demonstrated that the apparent distortion decreased toward the sea surface. The pattern that was evident at $z = 2.7$ m was still faintly discernible at a depth of 15.4 m (2/3 of the way from the seabed to the surface), but was absent at a depth 0.2 m. The location of the ADCP relative to the Cohasset production platform suggests that the platform legs were responsible for the flow distortion (see Anderson 1998).

At Hibernia, a comparison of the statistics of 2,544 hours of current records at the SE and NE current meter sites (Table 6) does not show any obvious dissimilarities between the two sites. The mean current vectors, principal axes orientation, and the variances of the current with respect to the principal axes are all very similar between the two Hibernia sites for all three years. Based on these statistics, it was concluded that the current regimes at the two sites were comparable, and that they may both be taken as representative of the general vicinity of the Hibernia GBS, approximately midway between them.

At both sites, the current regime is characterised by mean currents that are small relative to the variable components of the current (approximately 8-12 % in all except one year, Table 4 and Table 7). The variable components of the current, resolved on the principal axes of variation, are about equal in most years.

Little year-to-year variation is evident in the current statistics, with the exception of 1993 at Cohasset, where the direction of the mean current differs from that for 1995 and 1996. This anomaly is still evident when considering just the hours of the year when ADCP data was available for all three years, Table 5. In view of the weak magnitude of the mean current, the interannual variability in the direction is probably real.

6.2 Waves

The swell observed at Cohasset concurrent with ADCP data output in all three years was entirely non-breaking deep and intermediate-depth linear (Airy) waves (Figure 19 - Figure 21). Heights ranged up to 6 m, but were reported to be zero from 37 to 44 percent of the time (Table 8). Periods ranged from 4 to 18 s (Table 8), and wavelengths were from 25 to approximately 350 m. The wave height and period distributions were very similar in all three years.

At Hibernia, swell observed concurrent with current meter measurements (Figure 22 - Figure 24) was intermediate and deep water waves. Heights up to 8 m were reported, and periods ranged from 4 to 15 s. Some swell observations fell in the Stokes wave class in 1998 and 1999, but no breaking swell was reported. Calm seas were reported only 19 to 23 percent of the time (Table 9), in contrast to Cohasset (37 to 44 percent of the time). Table 9 indicates that the swell regime was stationary in the years of observation.

6.3 Shear velocities

Estimated bed shear velocities at Cohasset ranged up to 0.0705 m/s, about twice the maximum value (0.0342 m/s) at Hibernia, despite the higher waves observed there (Table 11 and Table 12). This difference may attributed to the greater depth at Hibernia (80 *vs.* 43 m), since the currents at Cohasset are not substantially greater than those at Hibernia.

The mean shear velocities at Cohasset ranged from 45 to 55% of the critical shear velocity for bedload transport initiation (Table 10), and were 21 to 38% greater than the those at Hibernia, which were from 37 to 40% of critical. Typical shear velocities ($u_{*cws\ mean} + u_{*cws\ std\ dev}$) were 98 to 99% of critical at Cohasset, but only 61 to 63 percent of critical at Hibernia, reflecting not only the lower mean stress at Hibernia, but also its smaller standard deviation.

6.4 Sediment transport

The sediment transport time series at both Cohasset (Figure 33 - Figure 35) and Hibernia (Figure 36 - Figure 38) show that sediment transport was highly discontinuous. The plots indicate that sediment transport occurs only when the shear velocity threshold u_{*crb} is exceeded.

The sediment transport at Cohasset exhibited extreme ranges in 1995 and 1996 due to the recording of 5.5 to 6.5 m swell on several occasions. These episodes were responsible for the large sediment transport maxima in 1995 and 1996, 1.52 and 8.47 m^2/s, respectively, 11 orders of magnitude greater than the transport minima in those years. (These large maxima were also responsible for skewing the means and standard deviations of the transports in those years.)

On the other hand, on two occasions (hour 600 of 1998, and hour 6400 of 1999), sediment transport did not occur at Hibernia during extreme current events because swell height was zero.

7 Conclusions

Observed near-seabed current and surface waves were used as input to a sediment transport model (SEDTRANS96) to evaluate (1) the combined wave-current seabed shear velocity and (2) the sediment transport response to the estimated seabed shear stress, at the Cohasset and Hibernia oil production sites. A sensitivity study showed that both near-seabed current and surface wave observations are needed to accurately predict bed stress, *i.e.*, significant errors could be expected if the stress were calculated using either current or wave observations alone.

It appears that at the Cohasset site, in the three years for which data were examined (1993, 1995, 1996), the near-seabed current measured by the ADCP was significantly distorted, possibly due to the proximity of two of the legs of the Cohasset production rig to the seabed-mounted ADCP instrument.

The current measurements from two sites within 3.8 km of the Hibernia GBS may be considered representative of the current around the GBS. The current measurements showed a weak mean

flow with a moderate variable component due to the tides, accompanied by larger secular current events.

8 Acknowledgements

The SEDTRANS96 program was developed under the auspices of the Geological Survey-Atlantic (GSCA, Natural Resources Canada). Michael Li of GSCA, BIO, provided the computer code for SEDTRANS96, and was most helpful with advice on its application.

The author would also like to acknowledge the assistance of John Loder, Bedford Institute of Oceanography (BIO), who initiated the project, and Yuri Geshelin, also of BIO, who made the Hibernia current meter data available. Terry Bullock, of AMEC Earth and Environmental, St. John's, NF, provided the MANMAR observations from Hibernia. Mark MacNeil, Kee Muschenheim, and Peter Smith contributed to the data assembly at Cohasset.

Ned King and Gary Sonnichsen of GSCA, and Tim Milligan of the DFO Habitat Ecology Division Particle Dynamics Laboratory at BIO assisted in interpreting the Hibernia seabed topography and sediments.

The creation of this Technical Report was funded by the Offshore Environmental Factors program of PERD.

9 References

Anderson, Carl, 1998. *Evaluation of Bottom Stress Variability on Sable Island Bank.* Contractor's Report, Contract F5955-6-0272, Challenger Oceanography, 18 March 1998.

Anderson, Carl, 2001. *Evaluation of Seabed Stress at the Hibernia Site, Grand Banks of Newfoundland.* Contractor's Report, Contract F5955-000470, Challenger Oceanography, 27 February 2001.

Bagnold, R.A., 1963. Mechanics of marine sedimentation. In: *The Sea*, M.N. Hill (ed.), Wiley Interscience, New York, Vol. 3, pp. 507-527.

Barrie, J.V., C.F.M. Lewis, G.B. Fader, and L.H. King, 1984. Seabed processes on the Northeastern Grand Banks of Newfoundland; modern reworking of relict sediments. *Mar. Geol.*, 57, 209-227.

Coastal Ocean Associates, 1997. *Assessment of 1992, 1993 and 1995 PanCanadian ADCP current meter data- Cohasset site.* Report for Bedford Institute of Oceanography, Dartmouth, N.S. COA Coastal Ocean Associates Inc., Dartmouth, N.S..

Coastal Ocean Associates, 1998. *Physical oceanographic data report: 1996 current meter data-Cohasset Site.* Prepared for PanCanadian Limited by COA Coastal Ocean Associates Inc., Dartmouth, N.S., March 1997.

Coastal Ocean Associates, 1999. *Summary Assessment of Pancanadian ADCP Current Meter Data 1992-1996.* COA Coastal Ocean Associates Inc., Dartmouth, N.S., April 1999.

Environment Canada, 1982. *MANMAR. Manual of Marine Weather Observing.* 6th ed. Environment Canada, Toronto, Ontario, Jan. 1982.

Geshelin, Yuri S., John W. Loder, and D. Kee Muschenheim, 2001. *Moored Current and Hydrographic measurements at Hibernia.* Canadian Data Report of Hydrography and Ocean Sciences (in preparation).

Grant, W.D. and O.S. Madsen, 1979. Combined wave and current interaction with a rough bottom. *J. Geophys Res.*, 84:1797-1808

Grant, W.D. and O.S. Madsen, 1982. Moveable bed roughness in unsteady oscillatory flow. *J. Geophys Res.*, 87:469-481.

Grant, W.D. and O.S. Madsen, 1986. The continental shelf bottom boundary layer. *Ann. Rev. Fluid Mech.*, 18:265-305.

Komar, Paul, 1976. *Beach Processes and Sedimentation.* Prentice-Hall Inc., Englewood Cliffs, N.J.

Li, Michael Z. and Carl L. Amos, 1997. *SEDTRANS96: Upgrade and Calibration of the GSC Sediment Transport Model.* Geological Survey of Canada-Atlantic, Bedford Institute of Oceanography, Open File 3512, 1997, 140 pp.

Tables

Location	Latitude	Longitude	Depth	No. hours of observations							
	N	W	(m)	1993	1994	1995	1996	1997	1998	1999	2000
Cohasset	43°51.0'	60°38.0'	43	1855	-	5899	5498	-	-	-	-
Hibernia	46° 45.0'	48° 46.9'	77 to 84	-	-	-	-	-	7567	8760	3847

Table 1 Summary of Cohasset and Hibernia current meter deployments, 1993-2000.

Year	Data coverage	Hours of data	Sampling interval (hr)	Measurement height above seabed (m)	Depth sounding (m)
1993	16 hrs 17 Jun - 12 hrs 18 Jun	21			
	12 hrs 10 Aug - 17 hrs 12 Aug	54			
	15 hrs 18 Aug - 20 hrs 20 Aug	54			
	18 hrs 26 Aug - 23 hrs 28 Aug	54	1.0	5.8	43
	13 hrs 01 Sep - 13 hrs 01 Sep	1			
	10 hrs 11 Sep - 15 hrs 13 Sep	54			
	13 hrs 28 Sep - 22 hrs 04 Dec	1617			
	Total hrs	1855			
1994	No data	0	-	-	-
1995	13 hrs 21 Mar - 12 hrs 06 Sep	4056			
	00 hrs 07 Sep - 13 hrs 18 Oct	998	1.0	2.7	43
	18 hrs 18 Oct - 22 hrs 22 Nov	845			
	Total hrs	5899			
1996	14 hrs 06 Mar - 07 hrs 22 May	1618			
	19 hrs 06 Jun - 22 hrs 09 Jun	76			
	11 hrs 11 Jun - 12 hrs 27 Jun	368	1.0	2.7	43
	23 hrs 27 Jun - 22 hrs 14 Aug	1152			
	14 hrs 29 Aug - 23 hrs 01 Dec	2266			
	Total hrs	5498			

Table 2 Details of Cohasset ADCP data coverage, 1993-1996. All times are UTC.

Deploy-ment	Position Latitude, Longitude	Data coverage	Sampling interval (hr)	Instrument height above seabed (m)	Depth sounding (m)
I	46° 43.3' N 48 ° 45.5' W	17 hrs 19 Feb 1998 - 16 hrs 05 Jun 1998	0.5	3.0	84
II	46° 45.7' N 48 ° 46.2' W	17 hrs 05 Jun 1998 - 09 hrs 25 Sep 1998	1.0	3.0	77
III	Same as II	12 hrs 25 Sep 1998 - 10 hrs 25 May 1999	1.0	3.0	77
IV	Same as II	15 hrs 25 May 1999 - 06 hrs 09 Jun 2000	1.0	3.0	78

Table 3 Details of Hibernia current meter deployments, 1998-2000. All times are UTC.

Variable	Units	1993	1994	1995	1996
n		1855	No measure-ments	5899	5498
z	m	5.8		2.7	2.7
$U(z)_{max}$	m/s	0.2509		0.3263	0.4974
$U(z)_{mean}$	m/s	0.0054		0.0058	0.0097
$\theta_{U\ mean}$	^oT	225		12	14
$\theta_{U\ principal}$	^oT	72		116	117
v'_{RMS}	m/s	0.0539		0.0659	0.1027
u'_{RMS}	m/s	0.0515		0.0570	0.0872

Table 4. Statistics of hourly ADCP near-seabed current measurements at Cohasset, in the years 1993-1996.

Variable	Units	1993	1994	1995	1996
n		1329	No measure-ments	1329	1329
z	m	5.8		2.7	2.7
$U(z)_{max}$	m/s	0.2509		0.2686	0.4374
$U(z)_{mean}$	m/s	0.0034		0.0032	0.0103
$\theta_{U\ mean}$	^oT	209		7	267
$\theta_{U\ principal}$	^oT	87		95	108
v'_{RMS}	m/s	0.0522		0.0548	0.1033
u'_{RMS}	m/s	0.0506		0.0603	0.0767

Table 5 Statistics of the ADCP near-seabed current measurements at Cohasset, for the hours in which there were data in all of the years 1993-1996 (13 hrs 28 September to 22 hrs 22 November, one day later in 1996, a leap year).

Variable	Units	SE 1998	NE 1999	NE 2000
n		2544	2544	2544
z	m	3	3	3
$U(z)_{max}$	m/s	0.2435	0.2493	0.2810
$U(z)_{mean}$	m/s	0.0125	0.0083	0.0093
$\theta_{U\,mean}$	^{o}T	334	297	312
$\theta_{U\,principal}$	^{o}T	118	113	109
v'_{RMS}	m/s	0.0705	0.0725	0.0811
u'_{RMS}	m/s	0.0599	0.0502	0.0641

Table 6. Statistics of hourly near-seabed current measurements at the Hibernia SE and NE sites, for the period of the measurements at the SE site (1700 hrs 19 Feb to 1600 hrs 5 June).

Variable	Units	1998	1999	2000
n		7567	8760	3847
z	m	3	3	3
$U(z)_{max}$	m/s	0.3423	0.4670	0.2810
$U(z)_{mean}$	m/s	0.0200	0.0095	0.0093
$\theta_{U\,mean}$	^{o}T	328	324	324
$\theta_{U\,principal}$	^{o}T	117	111	113
v'_{RMS}	m/s	0.0812	0.0818	0.0799
u'_{RMS}	m/s	0.0621	0.0600	0.0653

Table 7. Statistics of the combined hourly current time series at Hibernia in the years 1998-2000.

variable	units	1993	1994	1995	1996
n		619	No measure-ments	1090	1155
$H=0$	*% of time*	44		45	37
H_{max}	*m*	5.5		6.0	6.5
H_{min}	*m*	0.5		0.5	0.5
H_{mean}	*m*	1.71		1.33	1.29
H_{median}	*m*	1.50		1.0	1.0
$H_{std\ dev}$	*m*	0.88		0.81	0.75
T_{max}	*s*	13		18	16
T_{min}	*s*	4		4	3
T_{mean}	*s*	7.73		7.8	7.5
T_{median}	*s*	8.0		7	8
$T_{std\ dev}$	*s*	1.82		2.0	1.7
$\theta_{w\ mean}$	^oT	47		29	23
$\theta_{w\ median}$	^oT	50		40	30
$\theta_{w\ std\ dev}$	^{o}	55		66	77

Table 8. Statistics of 3-hourly Cohasset swell wave observations concurrent with ADCP measurements and with swell height greater than zero ($H > 0$), in the years 1993-1996.

Variable	Units	1998	1999	2000
n		2015	2357	984
$H=0$	*% of time*	20	19	23
H_{max}	*m*	8.0	7.0	6.5
H_{min}	*m*	0.5	0.5	0.5
H_{mean}	*m*	2.0	2.1	2.2
H_{median}	*m*	2.0	2.0	2.0
$H_{std\ dev}$	*m*	1.1	1.0	0.9
T_{max}	*s*	15	15	15
T_{min}	*s*	4	4	5
T_{mean}	*s*	8.6	9.0	9.2
T_{median}	*s*	8	9	9
$T_{std\ dev}$	*s*	1.6	1.5	1.3
$\theta_{w\ mean}$	^oT	247	270	259
$\theta_{w\ median}$	^oT	240	260	250
$\theta_{w\ std\ dev}$	^{o}	83	78	83

Table 9. Statistics of 3-hourly Hibernia GBS swell wave observations concurrent with nearby current measurements and with swell height greater than zero ($H > 0$), in the years 1998-2000.

Transport mode	Critical shear velocity	Value
Bed load	u_{*crb}	0.0137 m/s
Suspended load	u_{*crs}	0.0227 m/s
Sheet flow	u_{*up}	0.0529 m/s

Table 10 Critical shear velocities for medium sand with grain diameter GD = 0.00025 m.

observations	units	1993	1994	1995	1996
n		1855	No measure-ments	5899	5498
$u_{*cws\ max}$	m/s	0.0399		0.0678	0.0705
$u_{*cws\ mean}$	m/s	0.0064		0.0062	0.0076
$u_{*cws\ median}$	m/s	0.0042		0.0044	0.0062
$u_{*cws\ std\ dev}$	m/s	0.0065		0.0062	0.0059

Table 11. Statistics of estimated seabed shear velocity u_{*cws} at Cohasset, in the years 1993-1996.

observations	units	1998	1999	2000
n		7567	8760	3847
$u_{*cws\ max}$	m/s	0.0342	0.0276	0.0203
$u_{*cws\ mean}$	m/s	0.0051	0.0053	0.0055
$u_{*cws\ median}$	m/s	0.0045	0.0047	0.0050
$u_{*cws\ std\ dev}$	m/s	0.0035	0.0032	0.0029

Table 12. Statistics of estimated seabed shear velocity u_{*cws} at Hibernia, in the years 1998-2000.

Variable	Units	1993	1994	1995	1996
n		367	No measure-ments	1130	1577
V_{max}	m^2/s	$3.73x10^{-6}$		1.52	8.47
V_{min}	m^2/s	$2.75x10^{-10}$		$8.62x10^{-11}$	$3.58x10^{-10}$
V_{mean}	m^2/s	$5.75x10^{-8}$		0.0024	0.0153
V_{median}	m^2/s	$1.29x10^{-8}$		$1.11x10^{-8}$	$1.88x10^{-8}$
$V_{std\ dev}$	m^2/s	$3.06x10^{-7}$		0.0511	0.3520
$\theta_{V\ mean}$	^oT	209		27	331
$\theta_{V\ median}$	^oT	218		36	319
$\theta_{V\ std\ dev}$	^{o}	99		95	101

Table 13 Statistics of predicted volumetric rate of sediment transport at Cohasset, in the years 1993-1996.

Variable	Units	1998	1999	2000
n		206	186	73
V_{max}	m^2/s	$9.24x10^{-7}$	$3.44x10^{-7}$	$1.70x10^{-7}$
V_{min}	m^2/s	$3.82x10^{-9}$	$5.14x10^{-9}$	$3.37x10^{-9}$
V_{mean}	m^2/s	$6.21x10^{-8}$	$3.99x10^{-8}$	$4.77x10^{-8}$
V_{median}	m^2/s	$3.76x10^{-8}$	$2.90x10^{-8}$	$3.81x10^{-8}$
$V_{std\ dev}$	m^2/s	$1.05x10^{-7}$	$3.77x10^{-8}$	$3.52x10^{-8}$
$\theta_{V\ mean}$	^oT	307	321	268
$\theta_{V\ median}$	^oT	302	317	284
$\theta_{V\ std\ dev}$	^{o}	83	91	98

Table 14. Statistics of predicted volumetric rate of sediment transport at Hibernia, in the years 1998-2000.

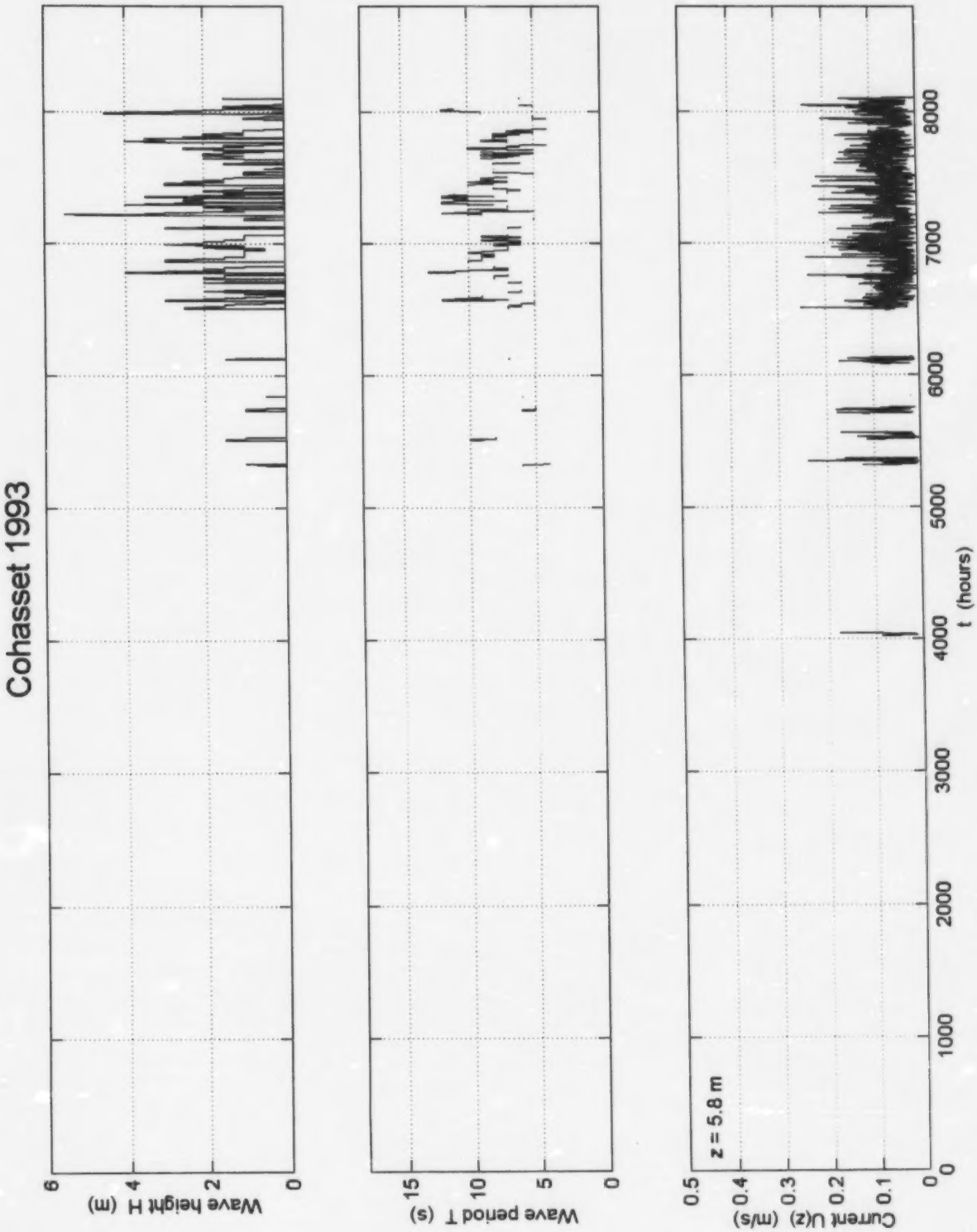

Figure 1. Hourly time series of swell height H, period T, and near-seabed current $U(z)$, at Cohasset, 1993.

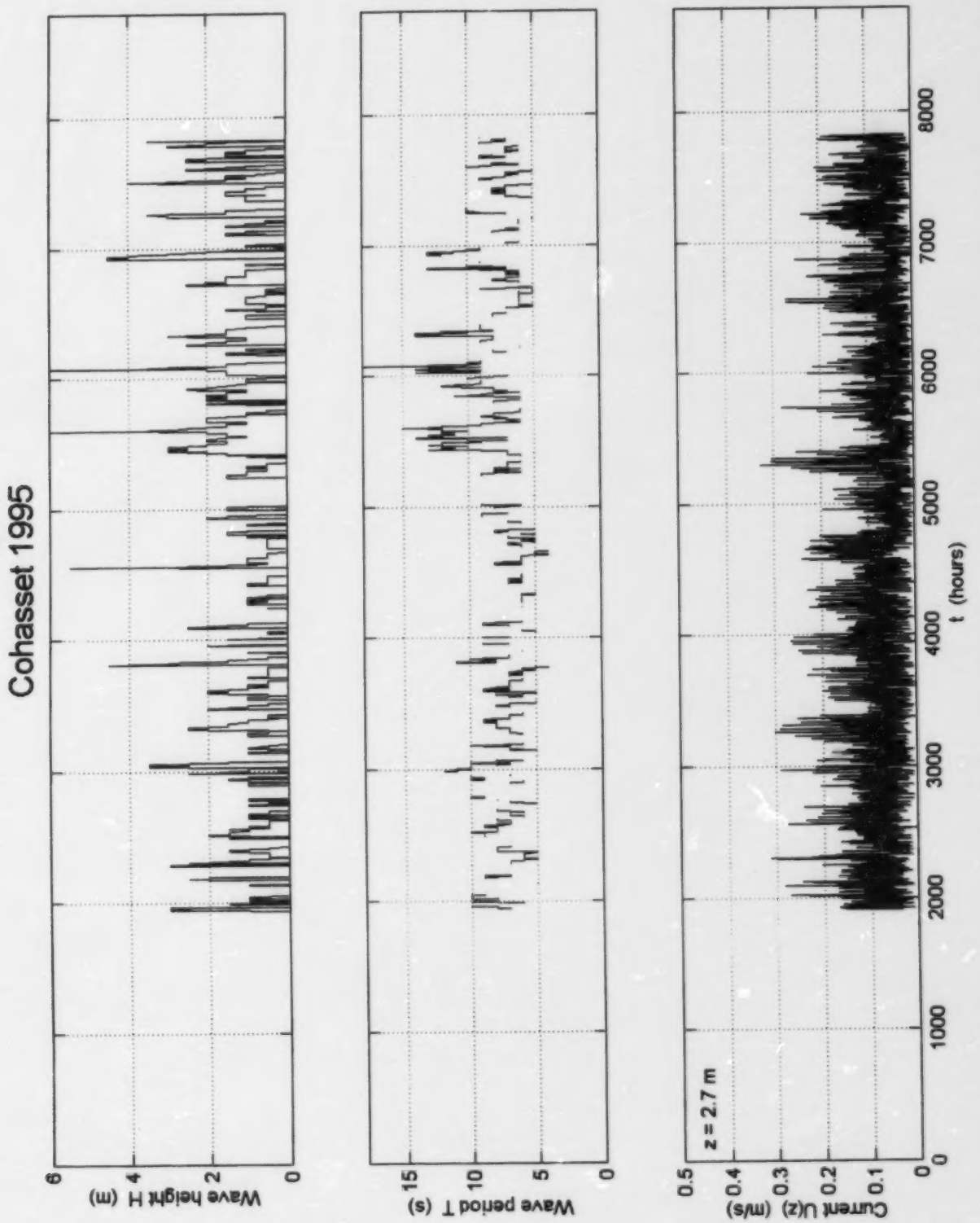

Figure 2. Hourly time series of swell height H, period T, and near-seabed current $U(z)$, at Cohasset, 1995.

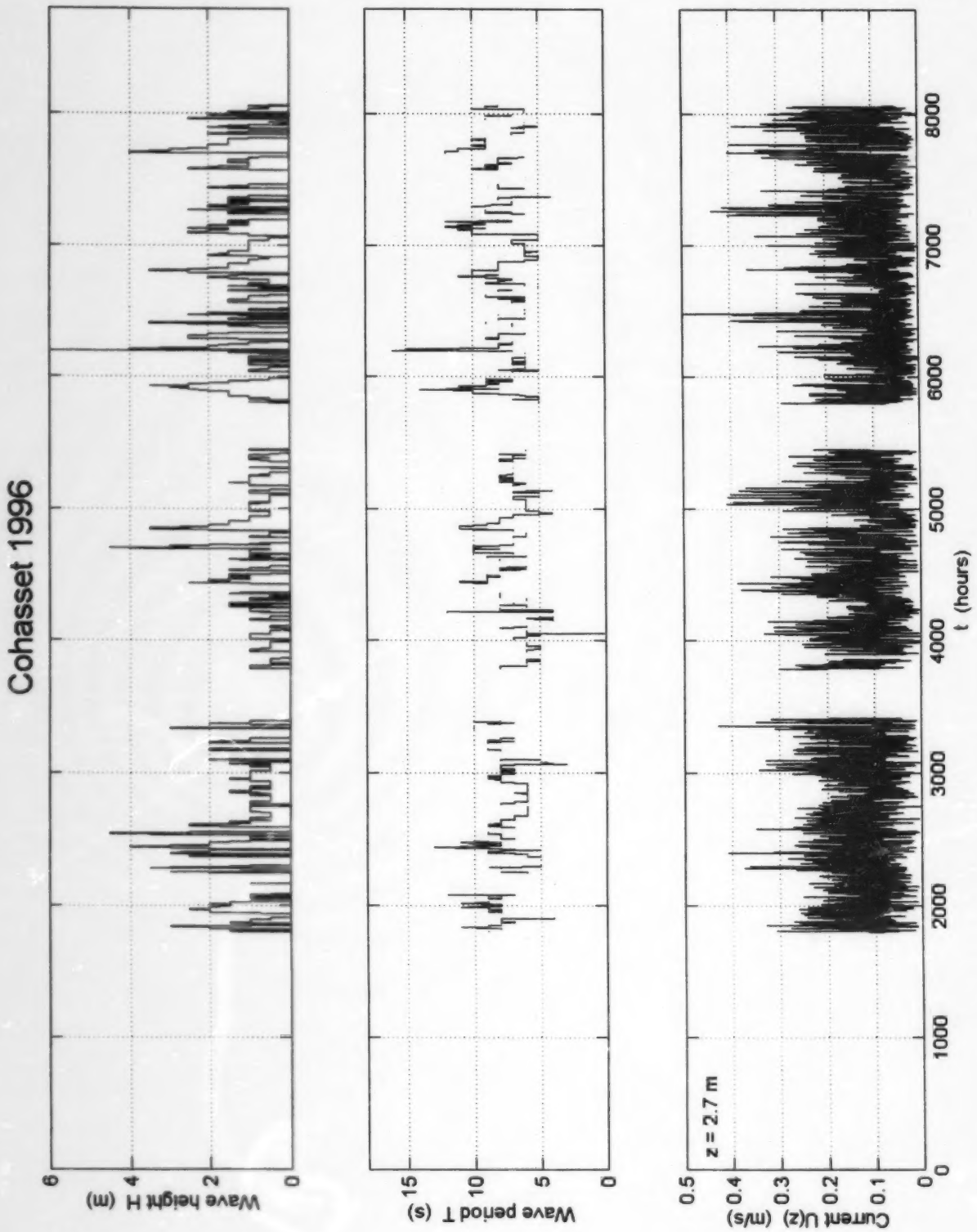

Figure 3. Hourly time series of swell height H, period T, and near-seabed current $U(z)$, at Cohasset, 1996.

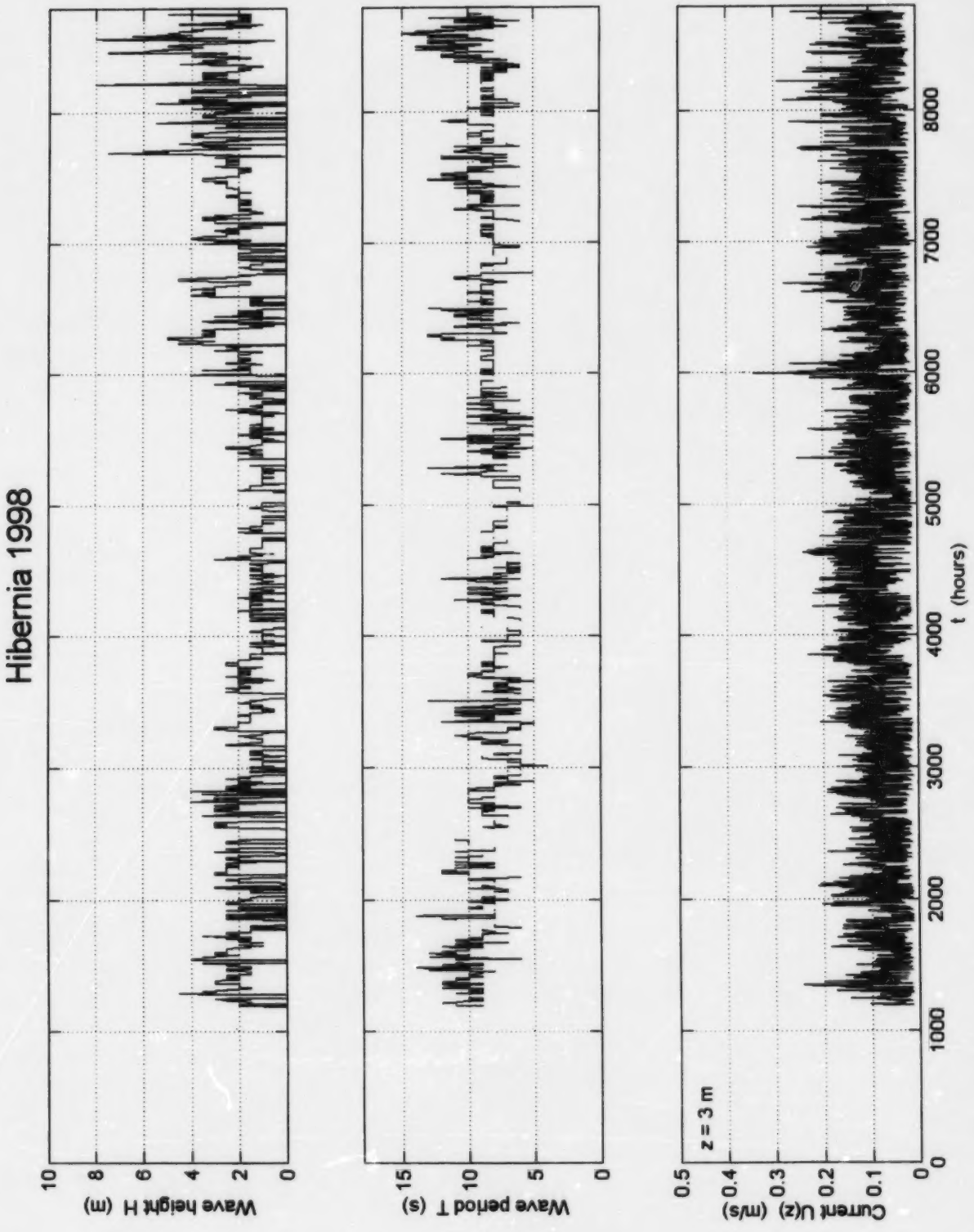

Figure 4. Hourly time series of swell height *H*, period *T*, and near-seabed current *U(z)*, at Hibernia, 1998.

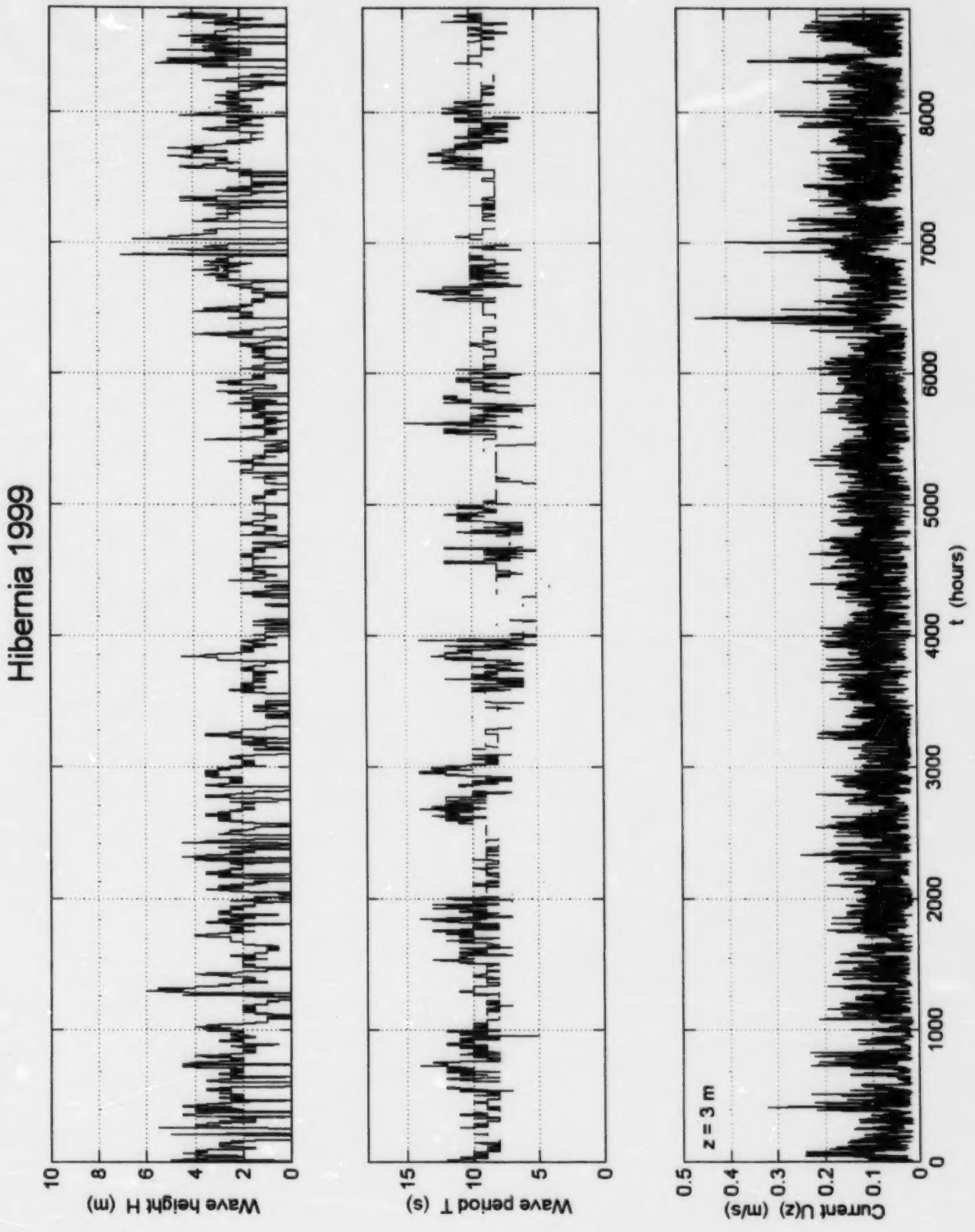

Figure 5. Hourly time series of swell height H, period T, and near-seabed current $U(z)$, at Hibernia, 1999.

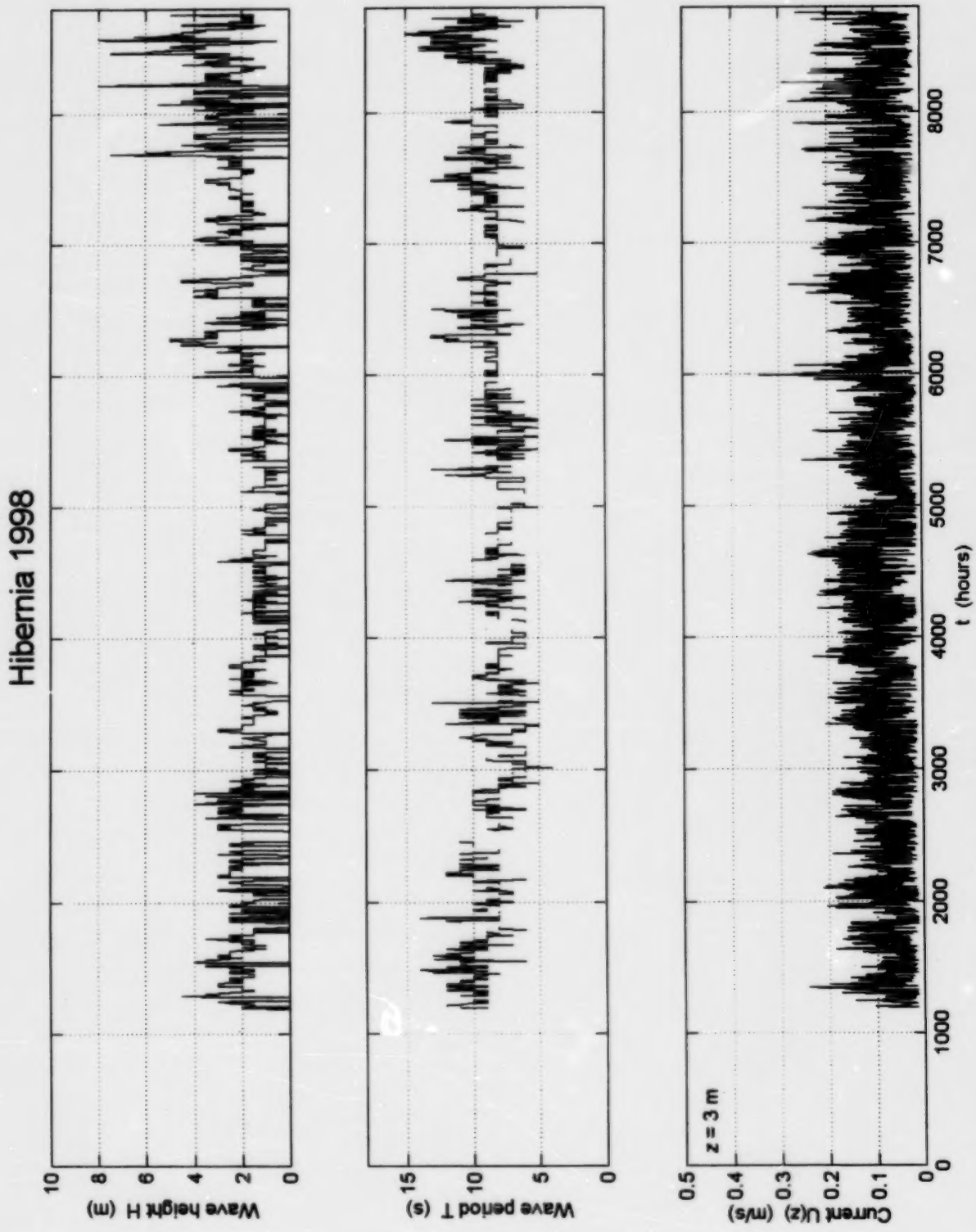

Figure 6. Hourly time series of swell height H, period T, and near-seabed current $U(z)$, at Hibernia, 2000.

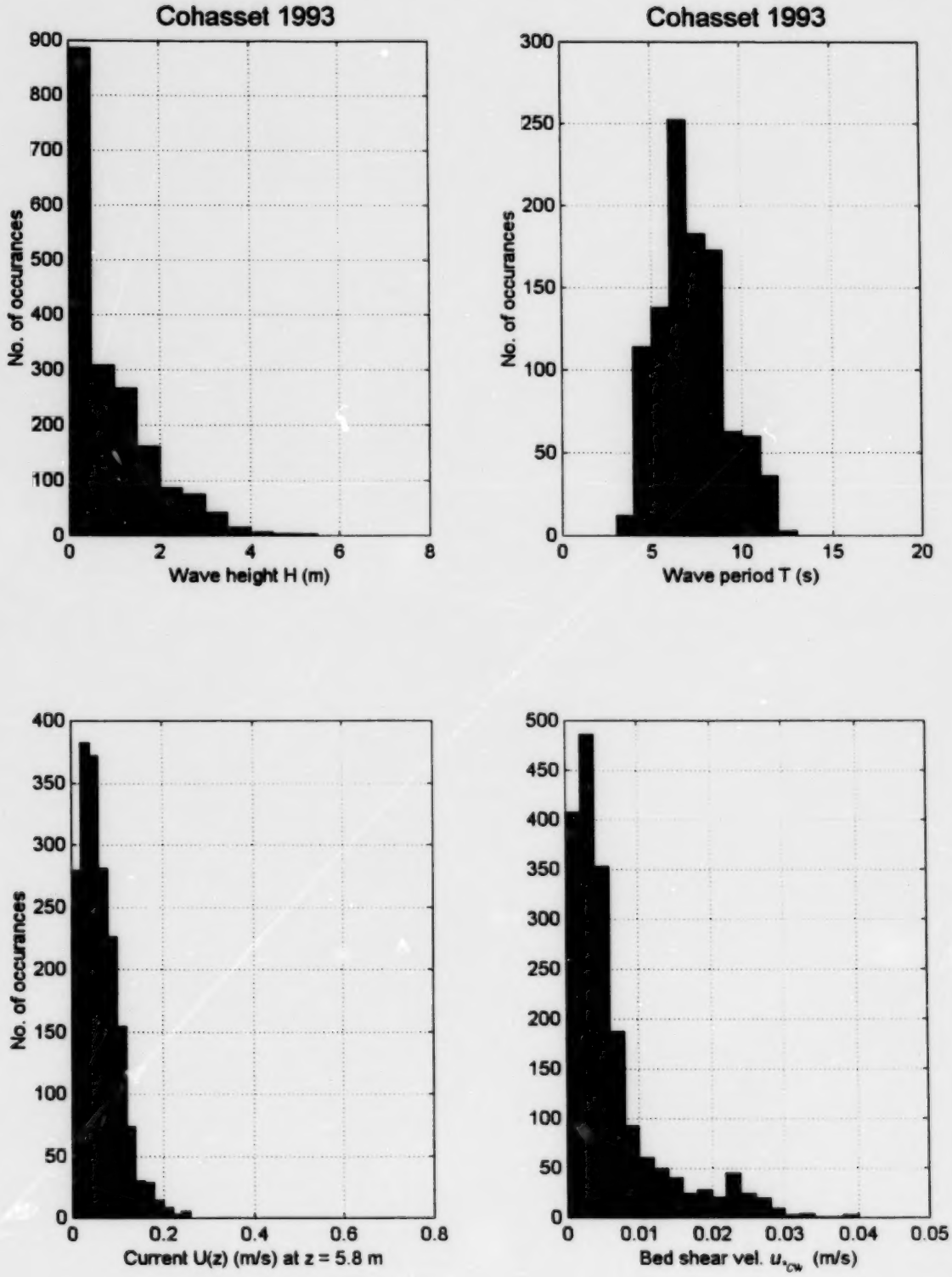

Figure 7. Histograms of hourly swell height H, period T, current magnitude $U(z)$, and skin-friction combined shear velocity u_{*cws} at Cohasset, 1993.

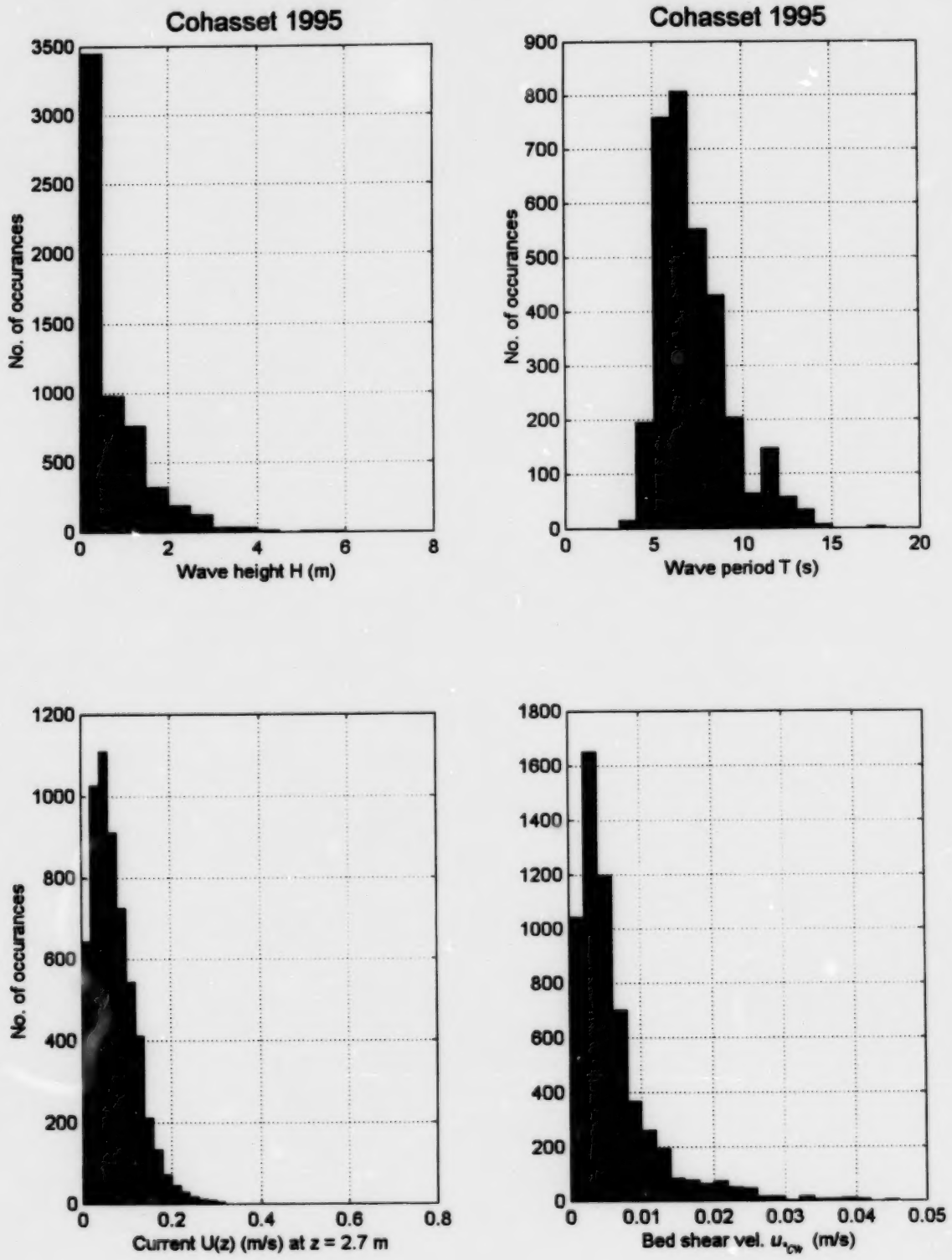

Figure 8. Histograms of hourly swell height H, period T, current magnitude $U(z)$, and skin-friction combined shear velocity $u_{*_{CWS}}$ at Cohasset, 1995.

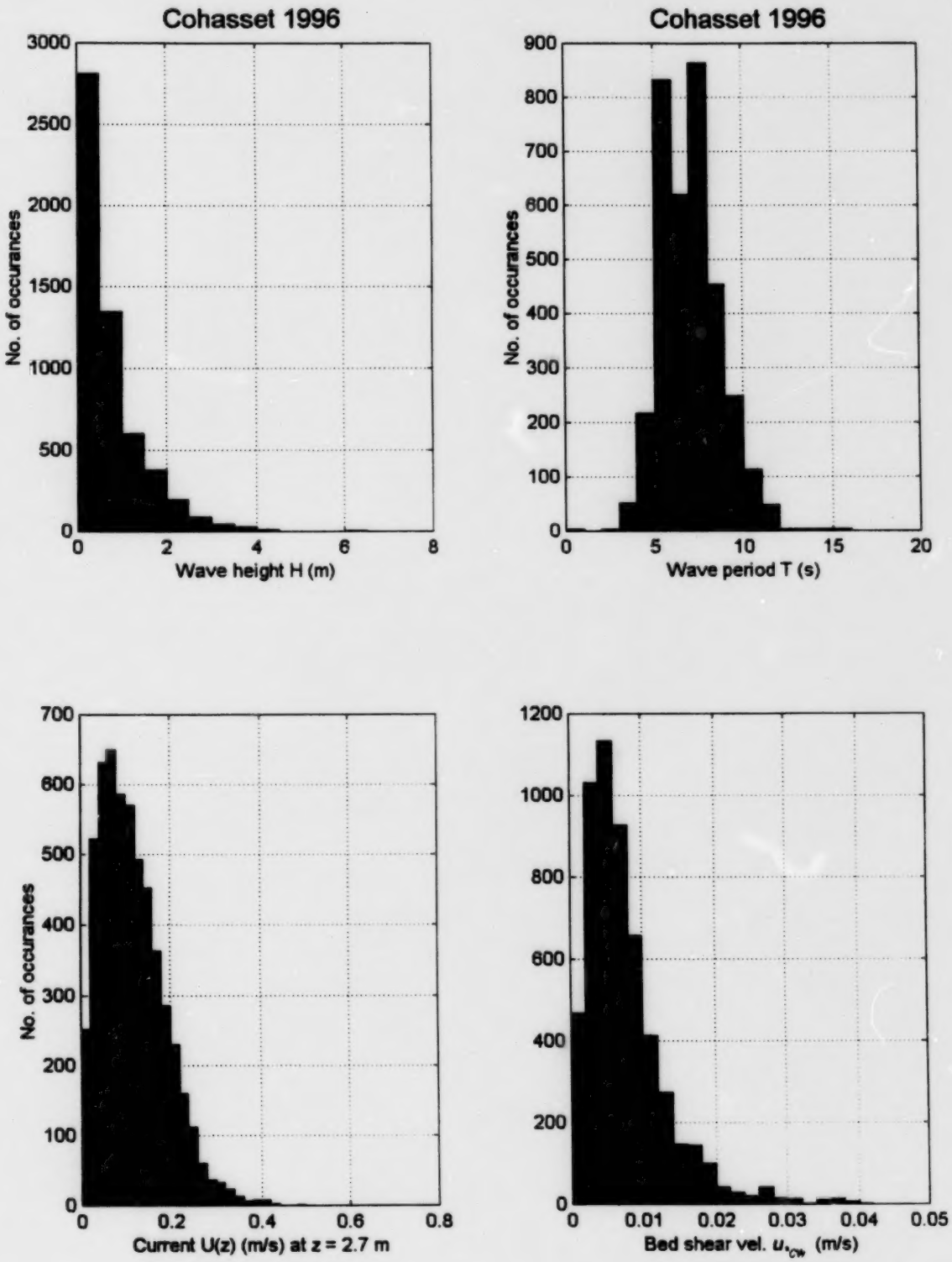

Figure 9. Histograms of hourly swell height H, period T, current magnitude $U(z)$, and skin-friction combined shear velocity $u_{*_{cws}}$ at Cohasset, 1996.

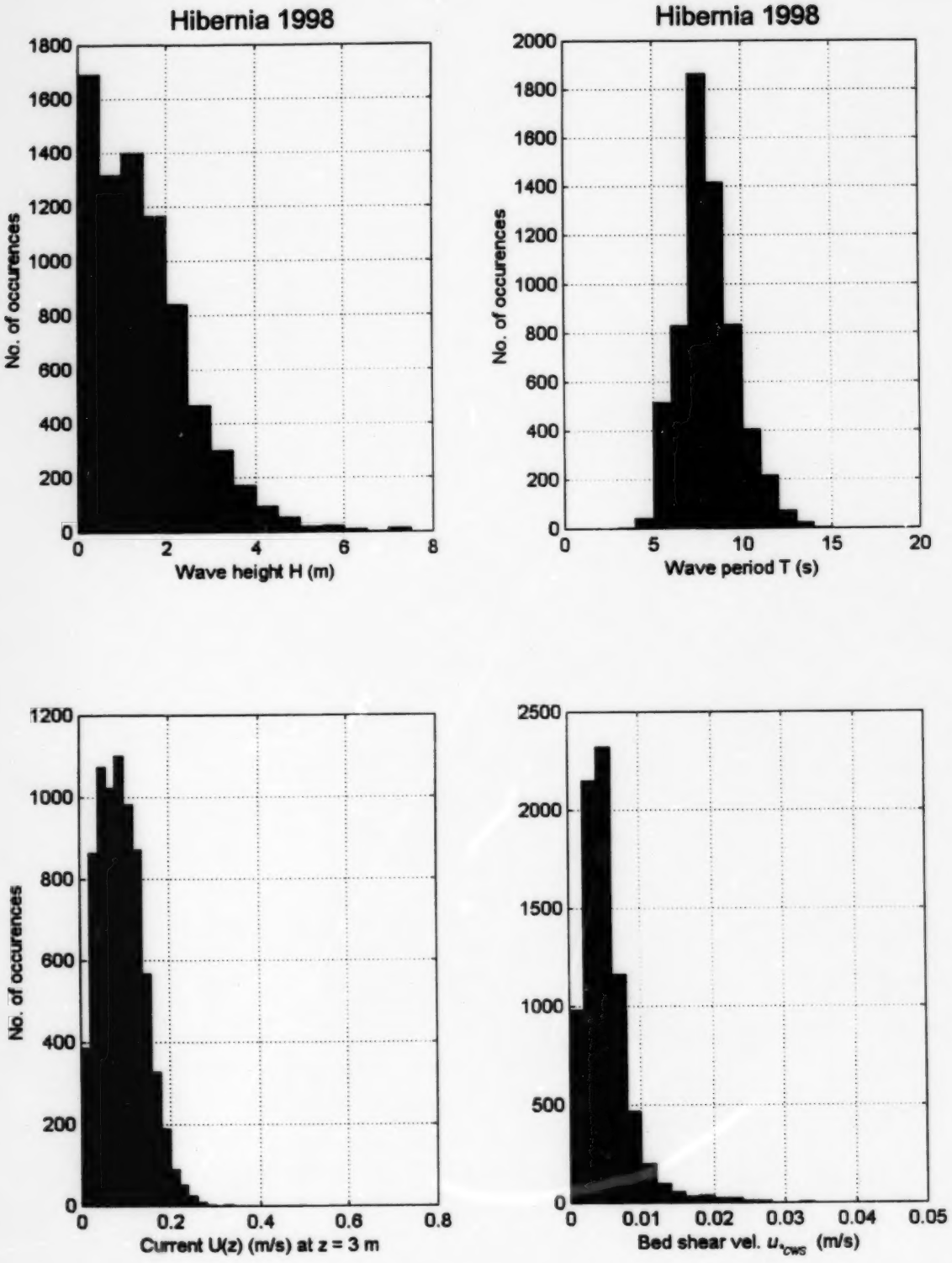

Figure 10. Histograms of hourly swell height H, period T, current magnitude $U(z)$, and skin-friction combined shear velocity u_{*cws} at Hibernia, 1998.

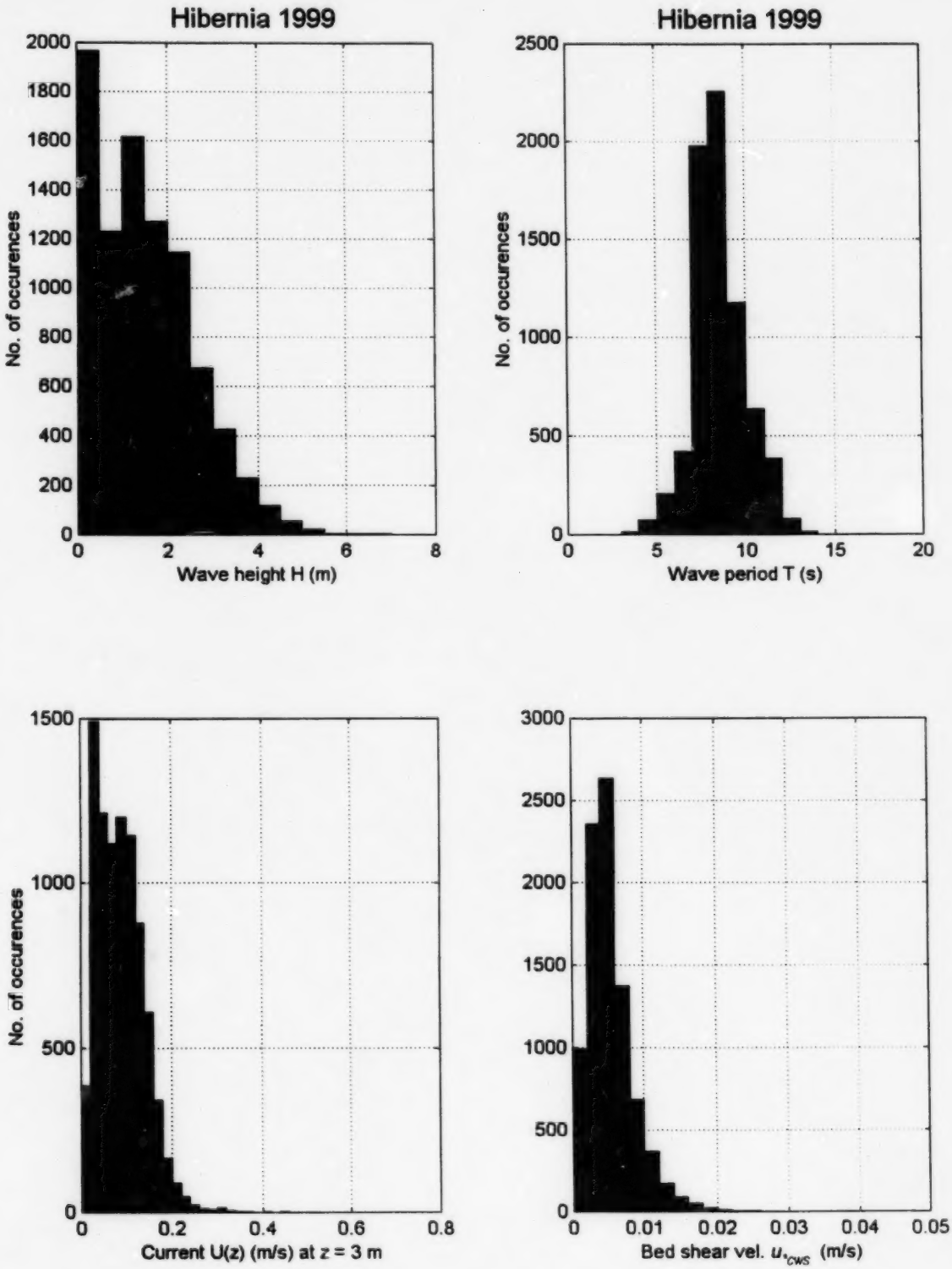

Figure 11. Histograms of hourly swell height H, period T, current magnitude $U(z)$, and skin-friction combined shear velocity u_{*cws} at Hibernia, 1999.

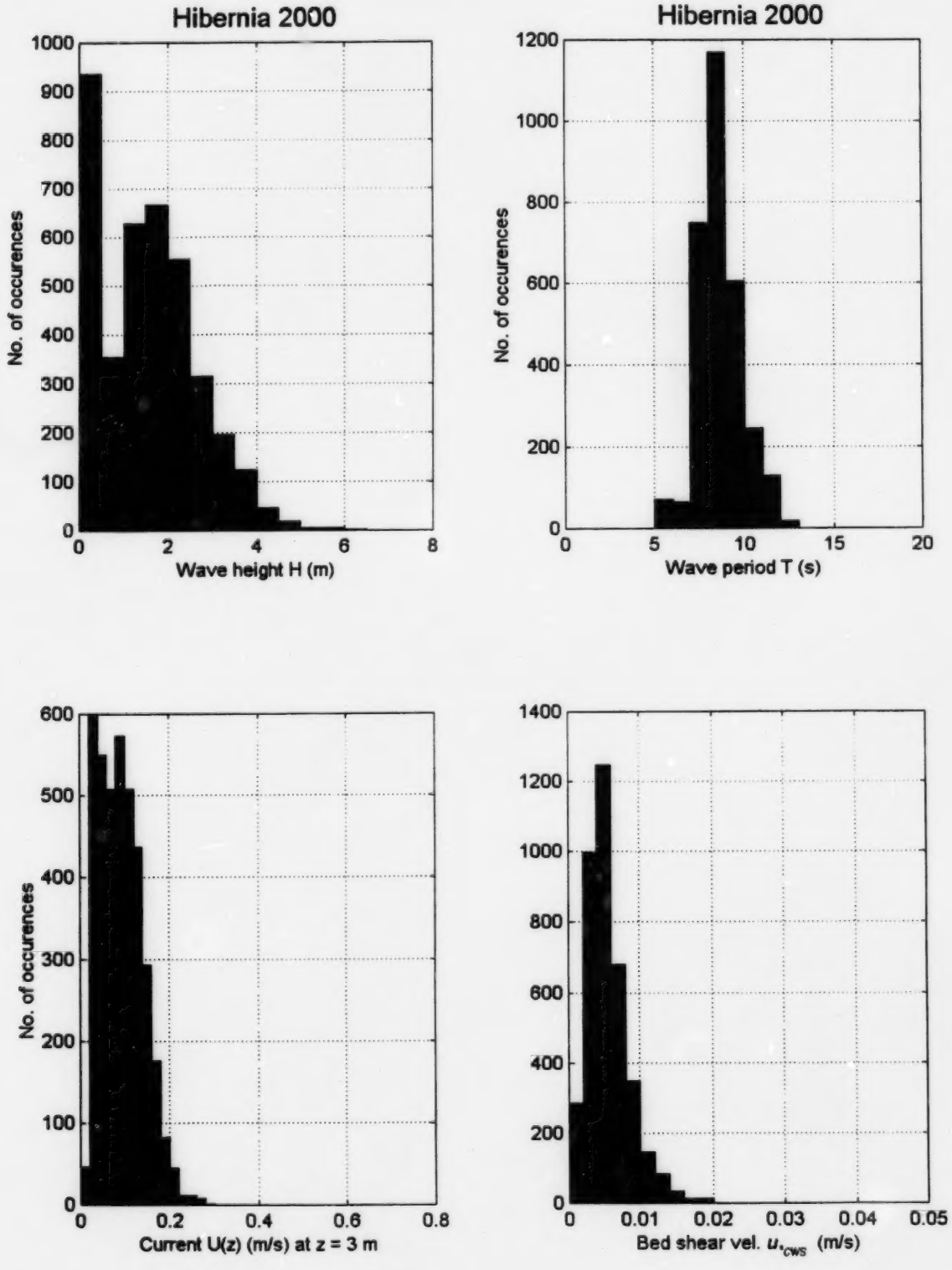

Figure 12. Histograms of hourly swell height H, period T, current magnitude $U(z)$, and skin-friction combined shear velocity u_{*cws} at Hibernia, 2000.

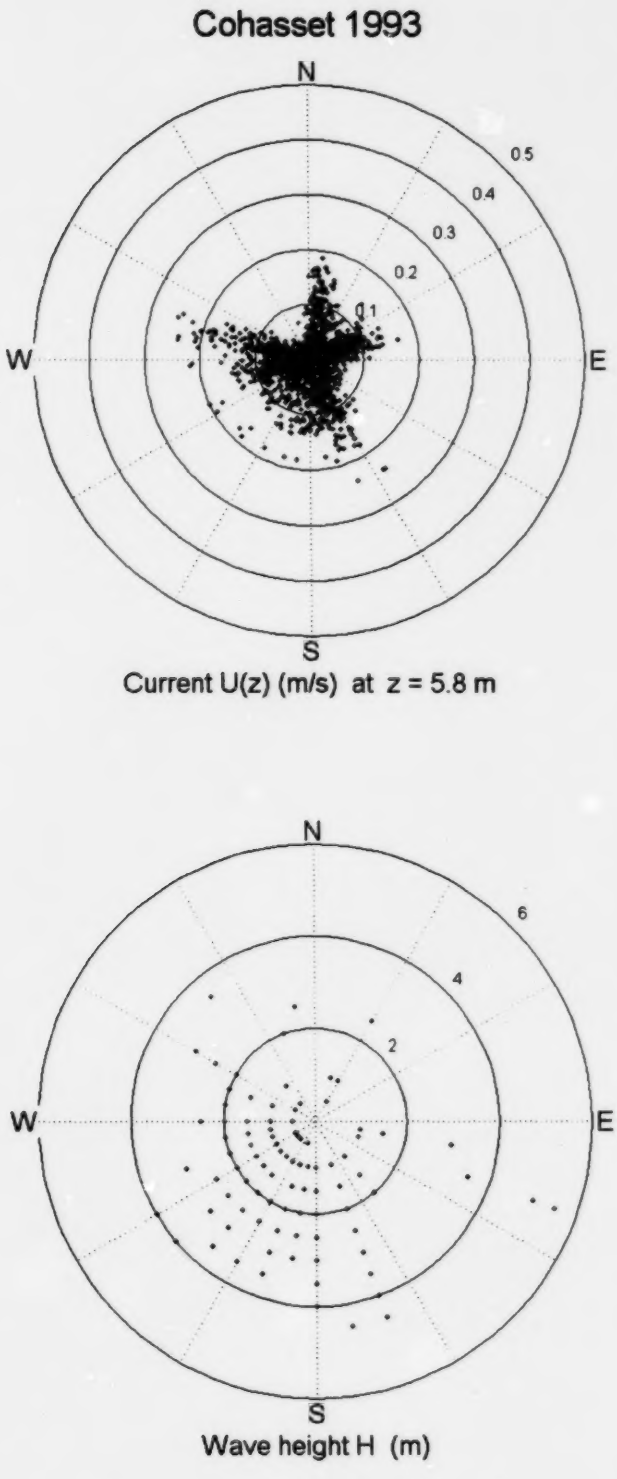

Figure 13. Polar plots of hourly near-seabed current *U(z)* magnitude versus current direction (toward), and hourly swell height *H* versus swell direction (from) at Cohasset, 1993.

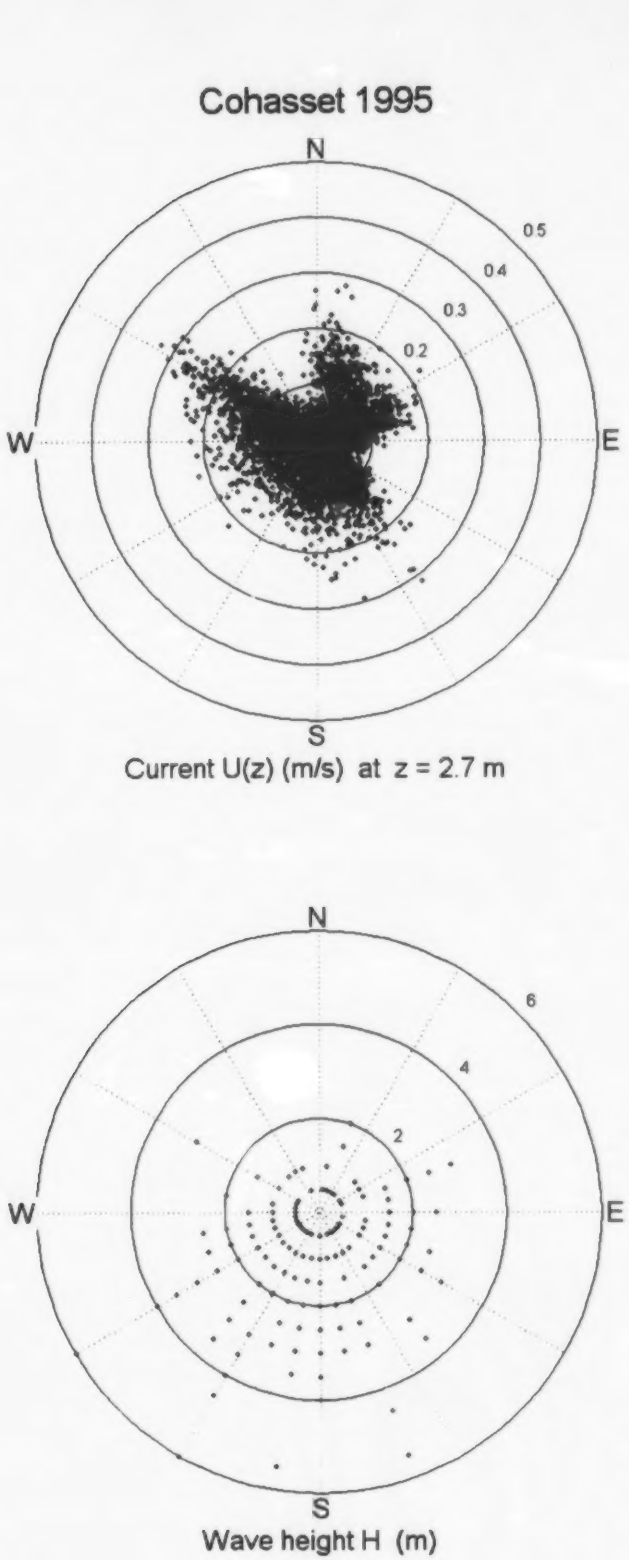

Figure 14. Polar plots of hourly near-seabed current *U(z)* magnitude versus current direction (toward), and hourly swell height *H* versus swell direction (from) at Cohasset, 1995.

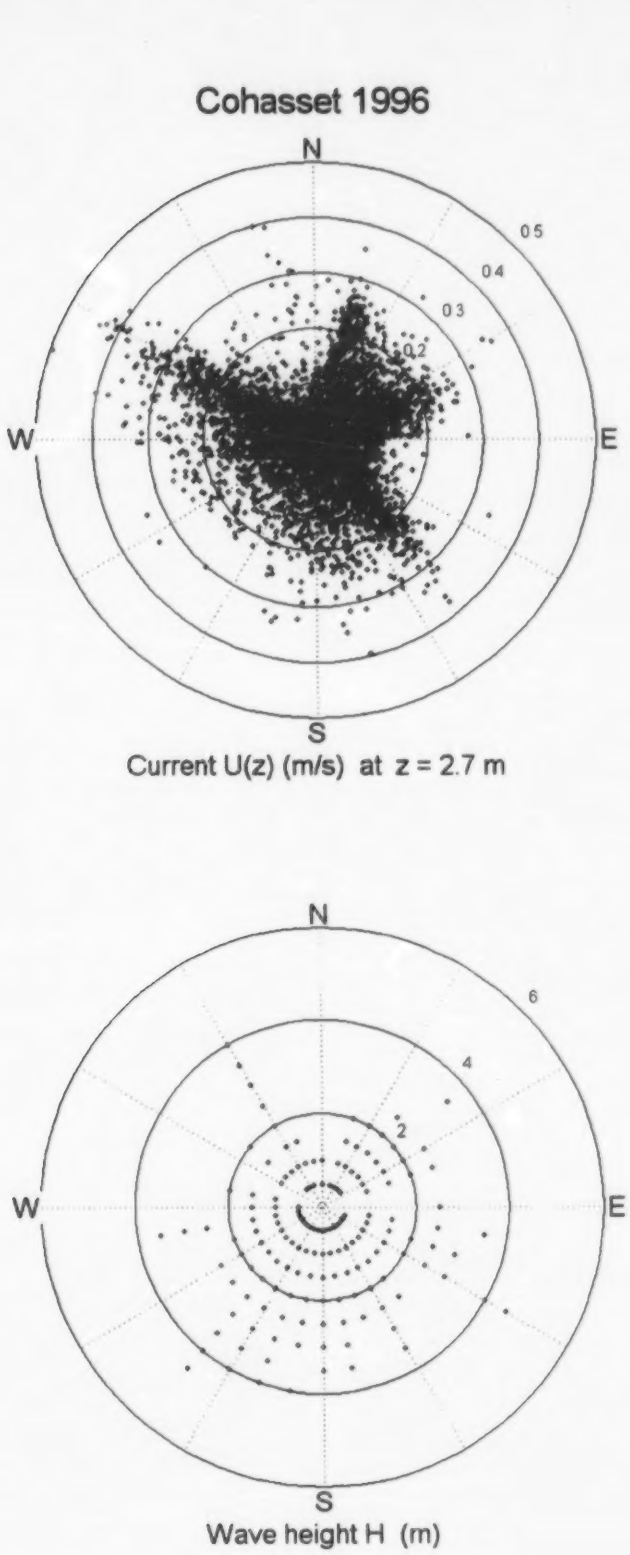

Figure 15. Polar plots of hourly near-seabed current *U(z)* magnitude versus current direction (toward), and hourly swell height *H* versus swell direction (from) at Cohasset, 1996.

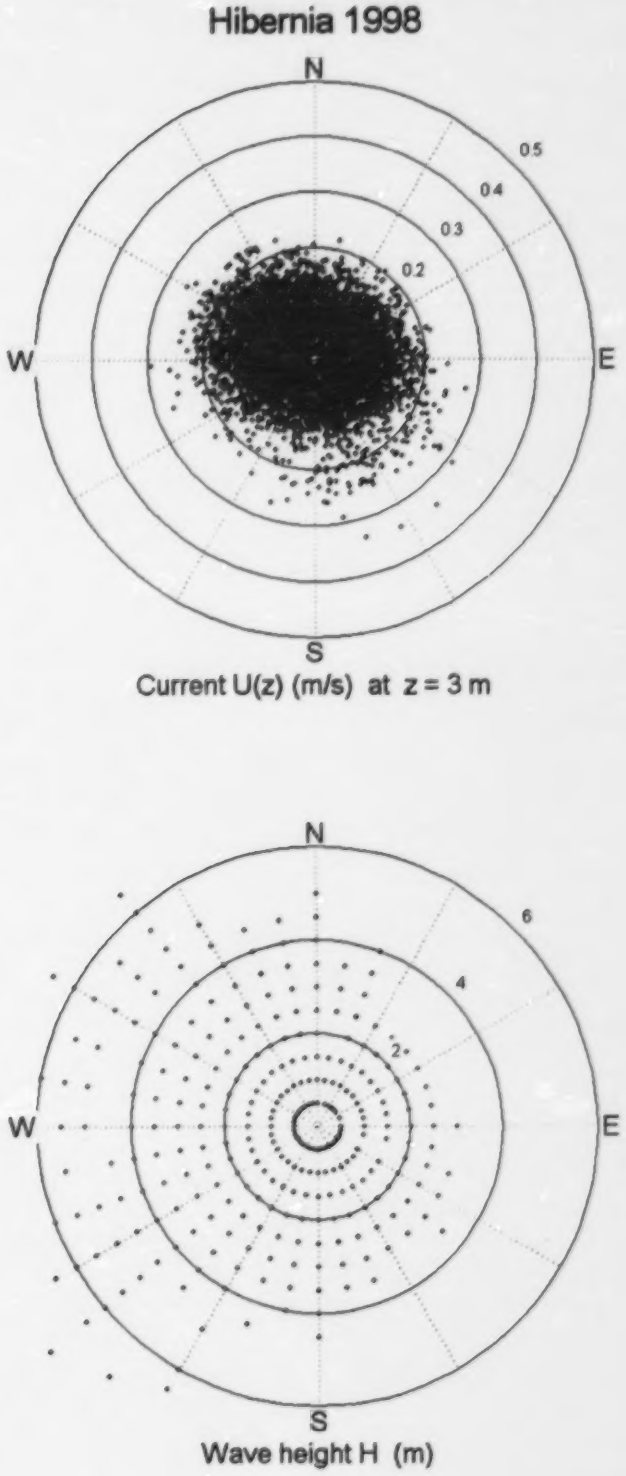

Figure 16. Polar plots of hourly near-seabed current *U(z)* magnitude versus current direction (toward), and hourly swell height *H* versus swell direction (from) at Hibernia, 1998.

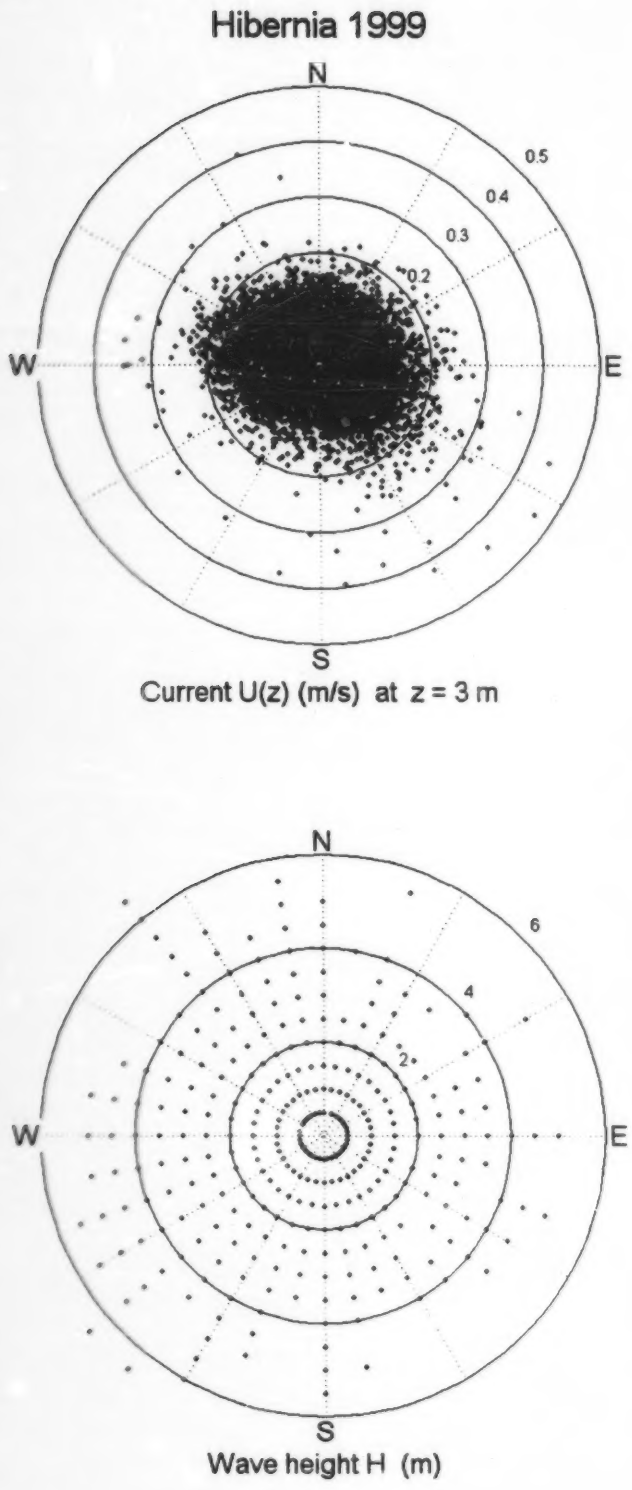

Figure 17. Polar plots of hourly near-seabed current *U(z)* magnitude versus current direction (toward), and hourly swell height *H* versus swell direction (from) at Hibernia, 1999.

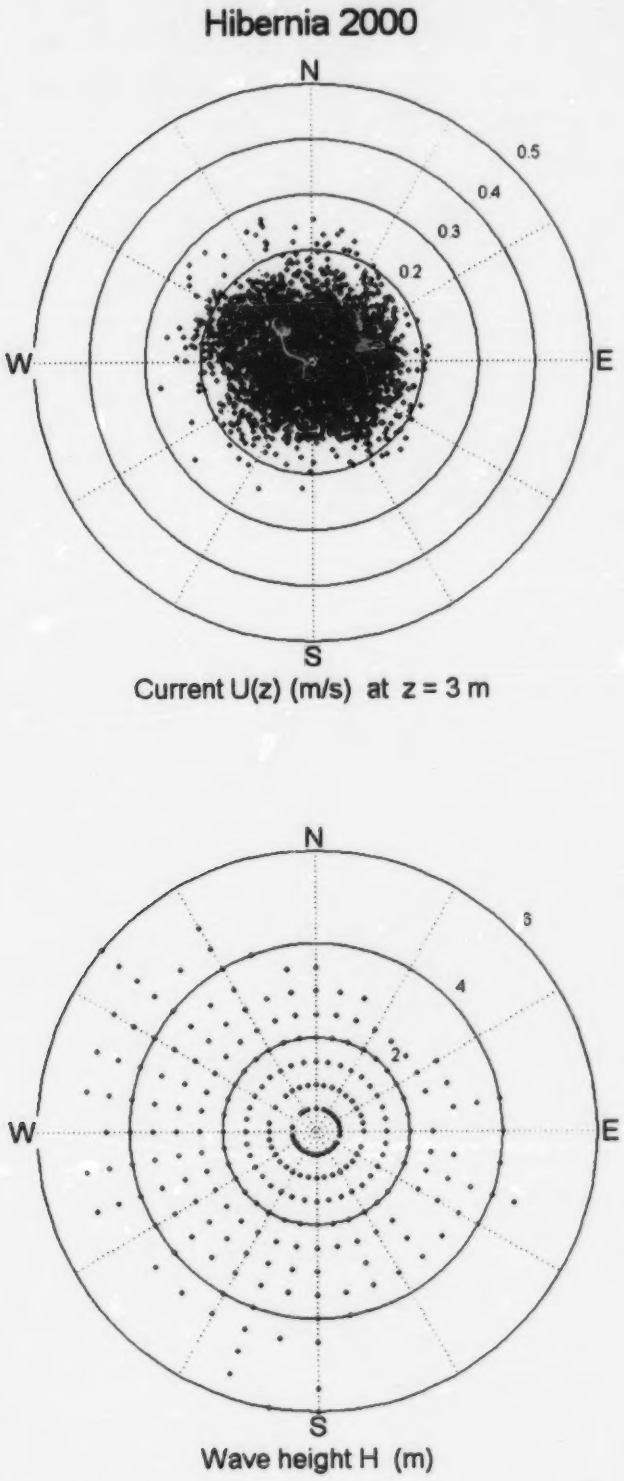

Figure 18. Polar plots of hourly near-seabed current *U(z)* magnitude versus current direction (toward), and hourly swell height *H* versus swell direction (from) at Hibernia, 2000.

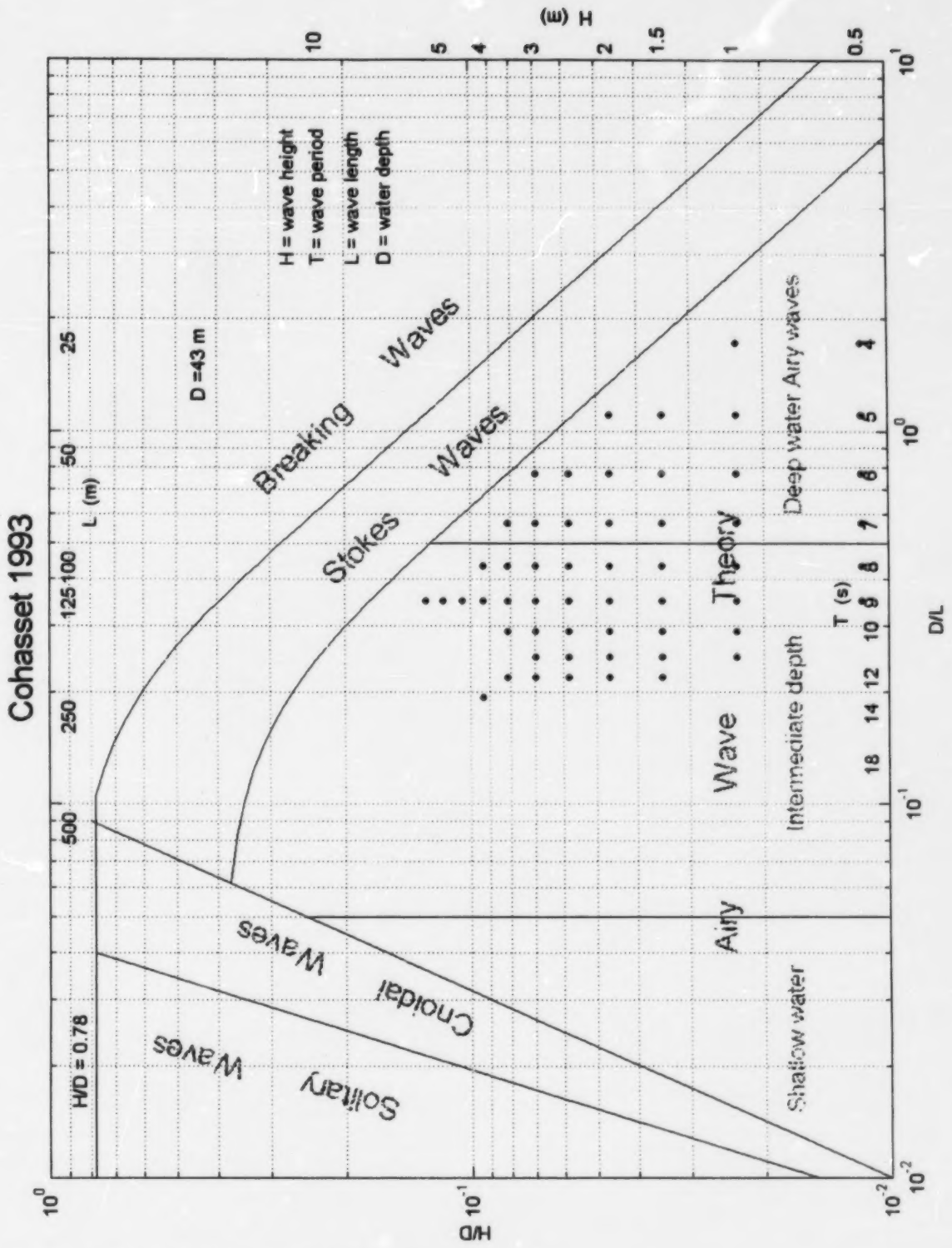

Figure 19. Wave types observed at Cohasset, 1993.

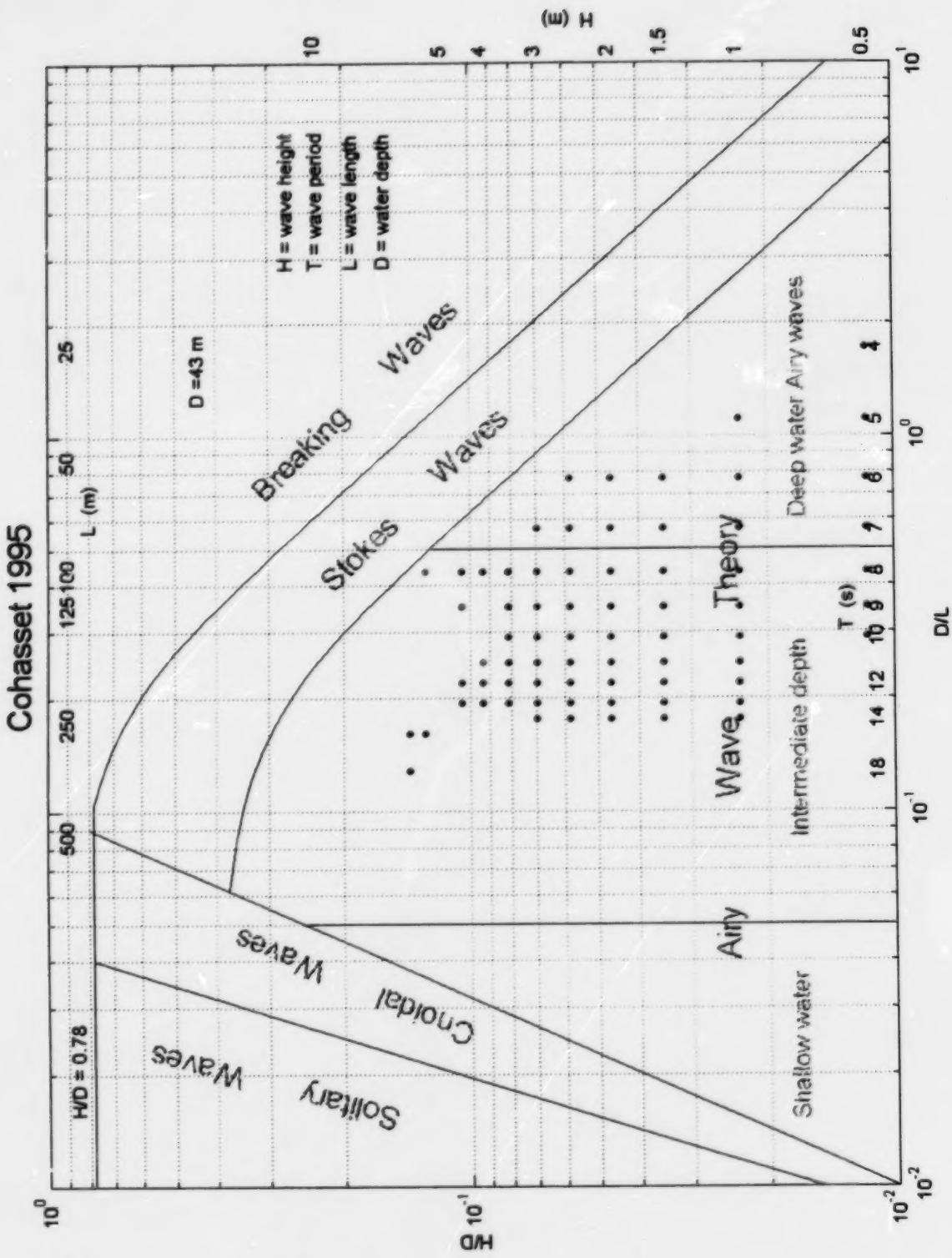

Figure 20. Wave types observed at Cohasset, 1995.

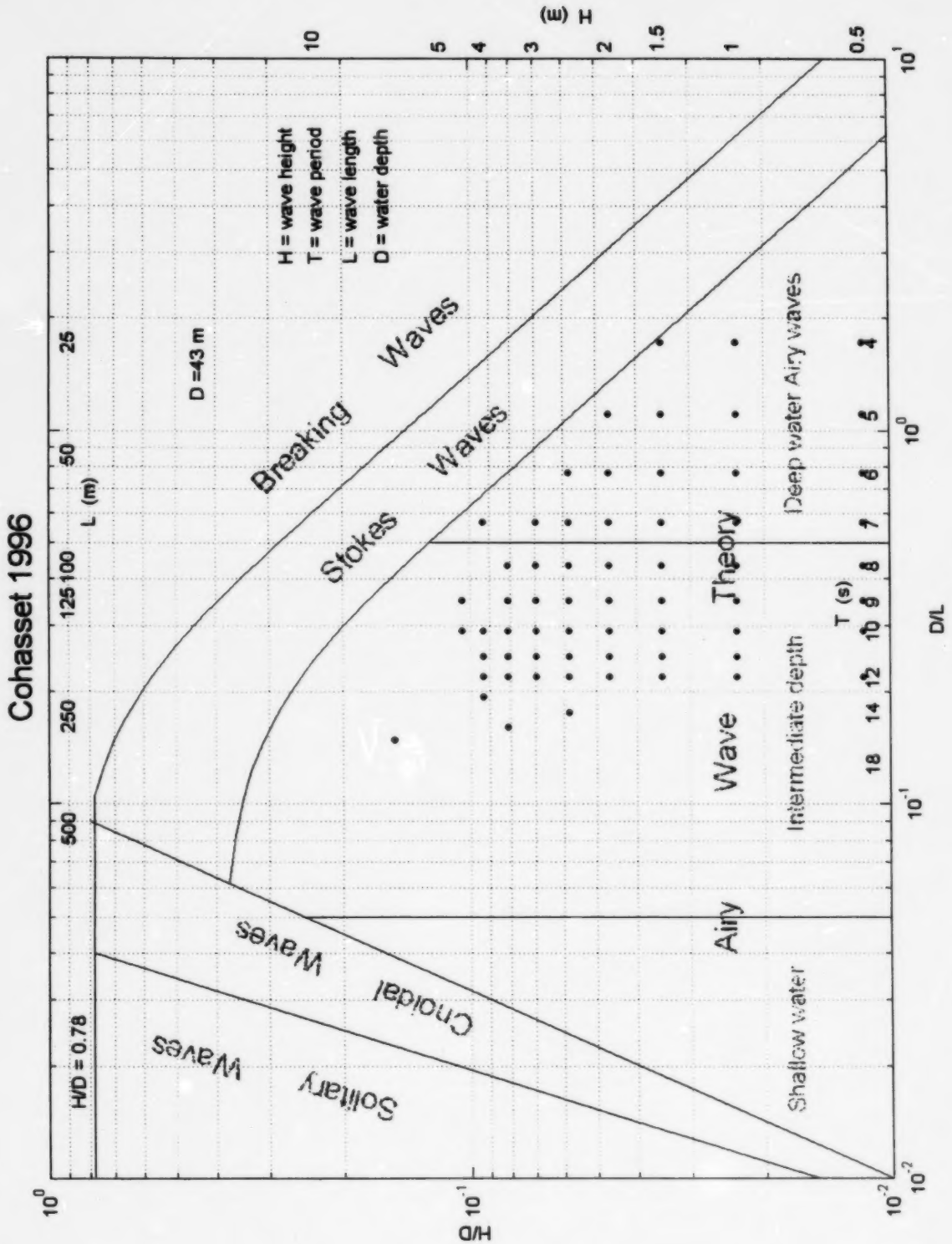

Figure 21. Wave types observed at Cohasset, 1996.

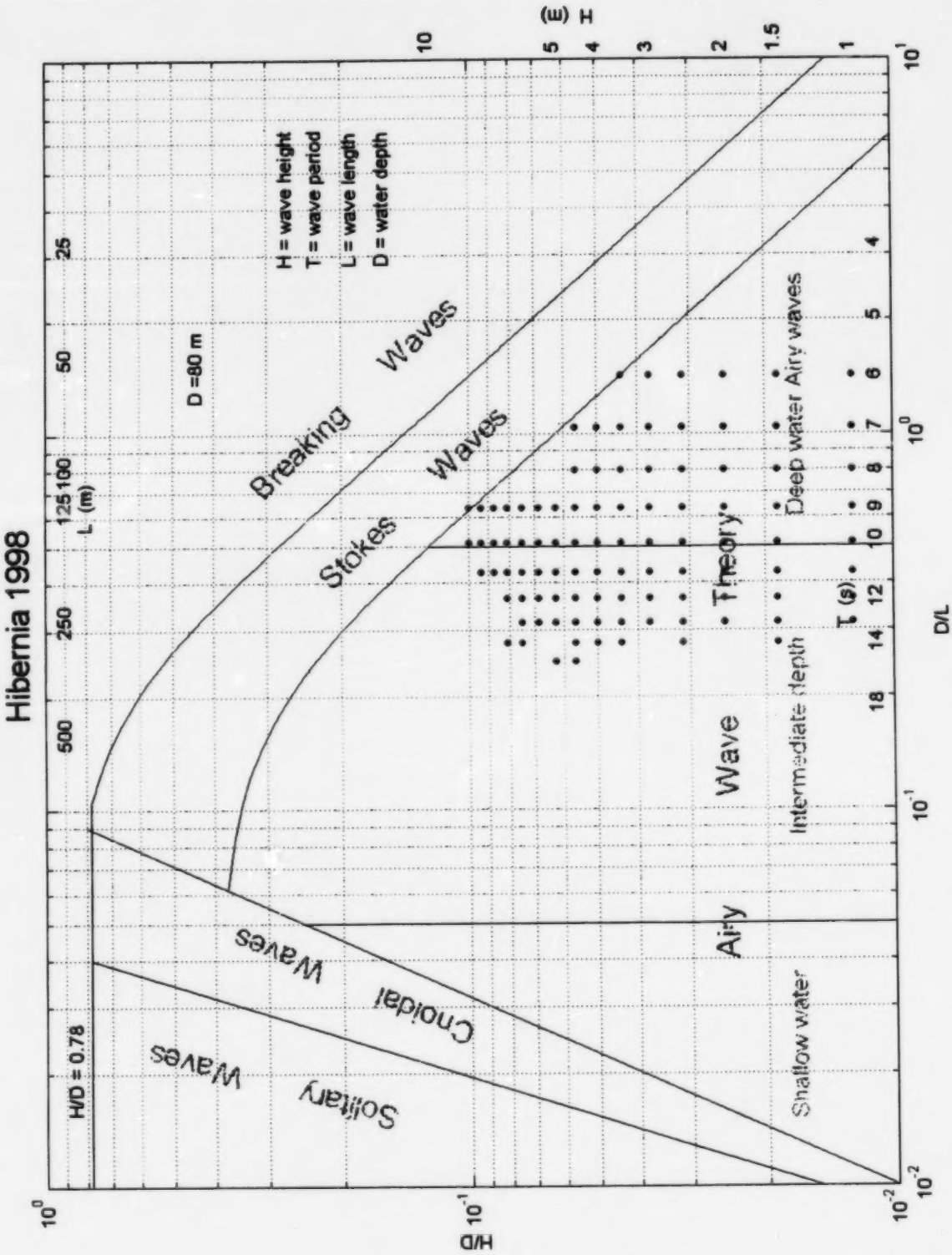

Figure 22. Wave types observed at Hibernia, 1998.

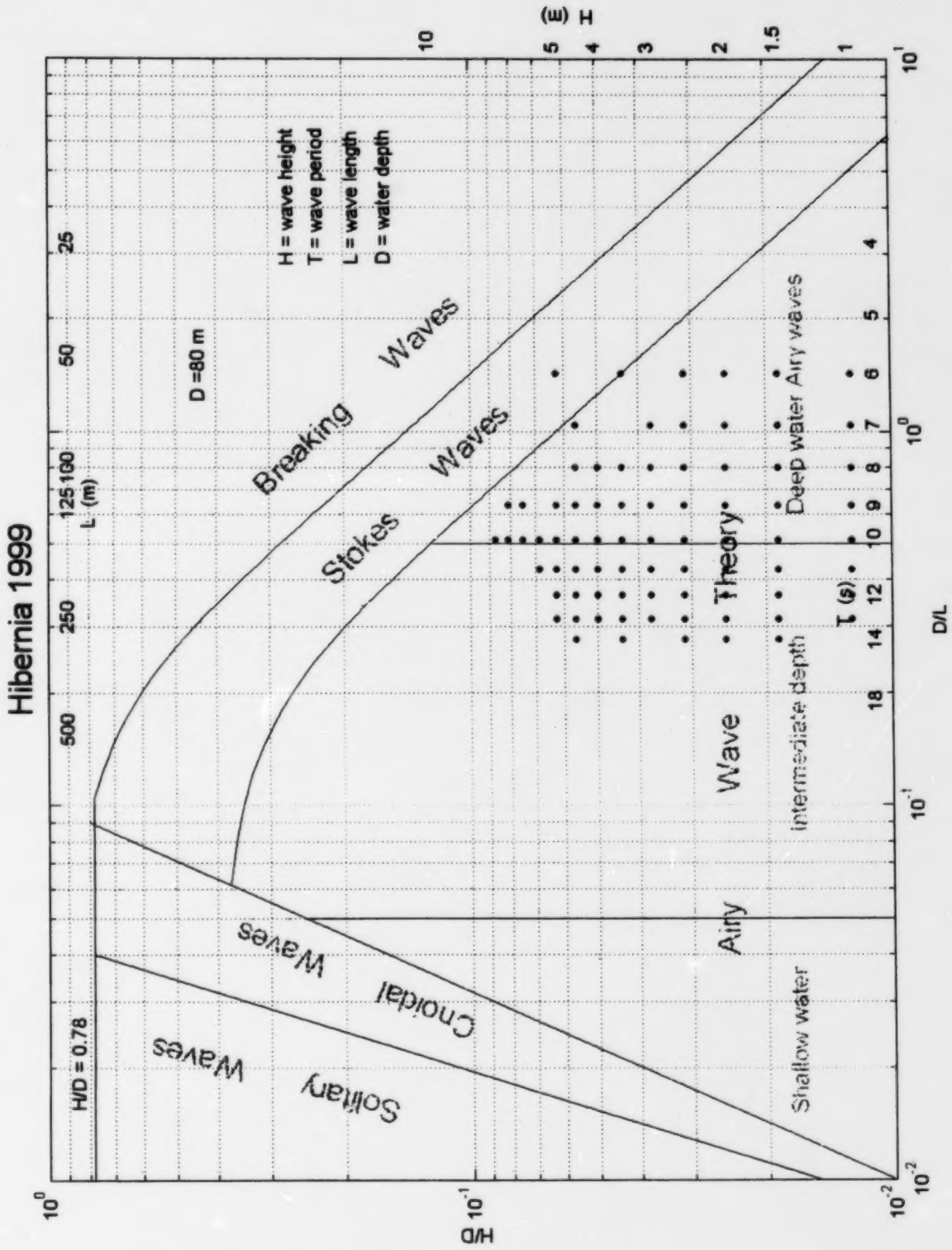

Figure 23. Wave types observed at Hibernia, 1999.

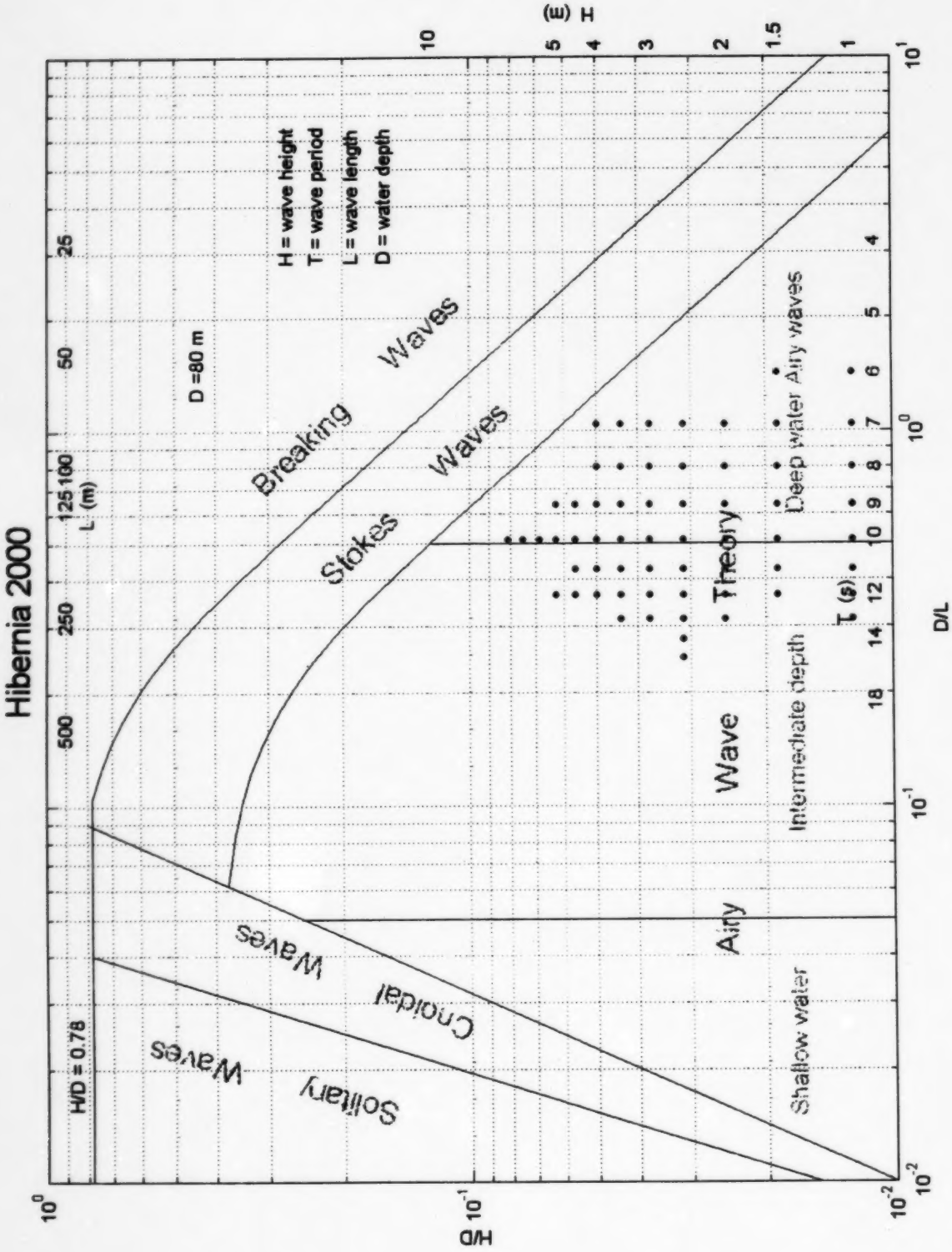

Figure 24. Wave types observed at Hibernia, 2000.

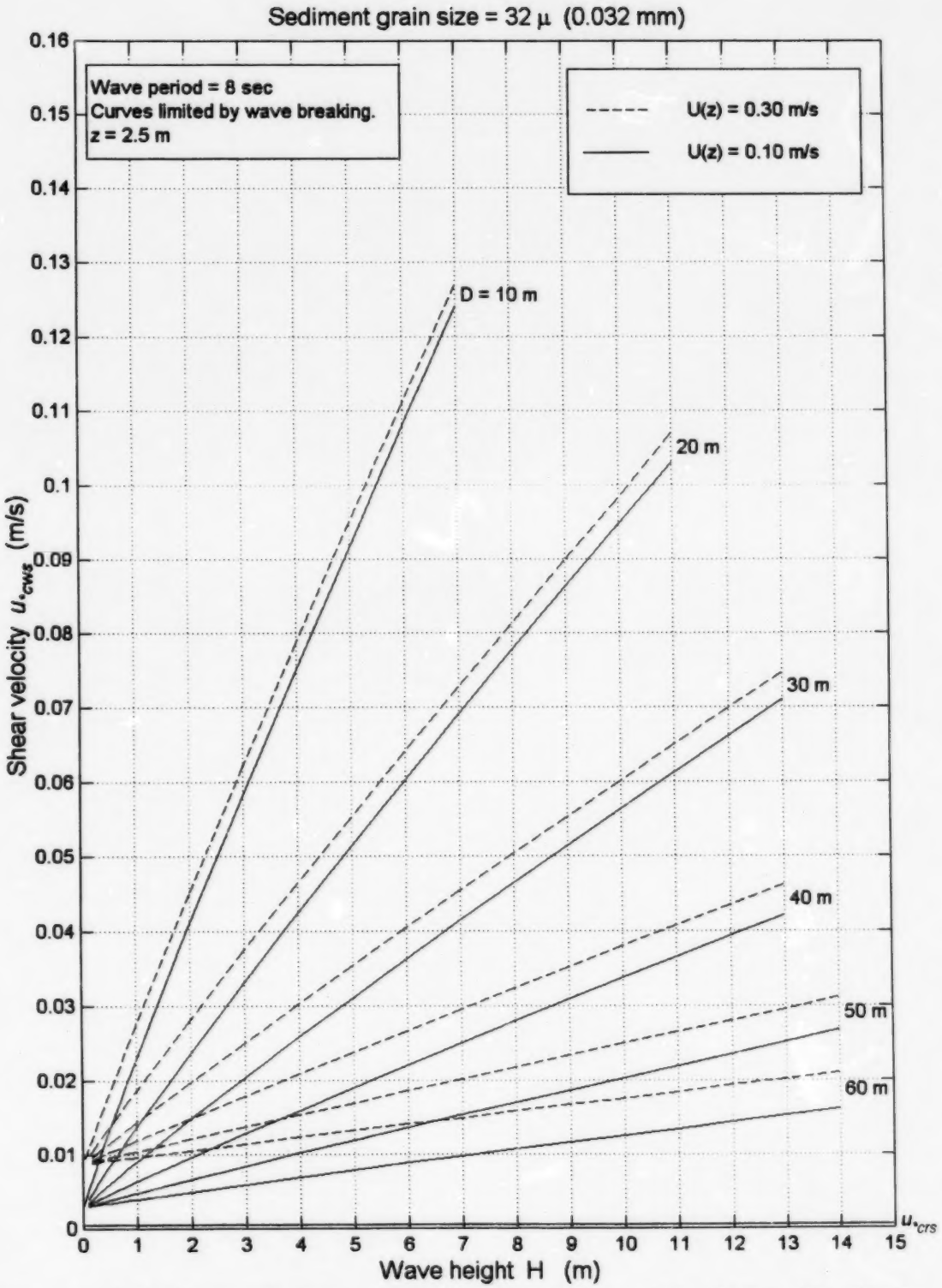

Figure 25. Seabed shear velocity u_{*cws} versus wave height for water depths from 10 to 60 m and sediment grain diameter 32μ (0. 032 mm).

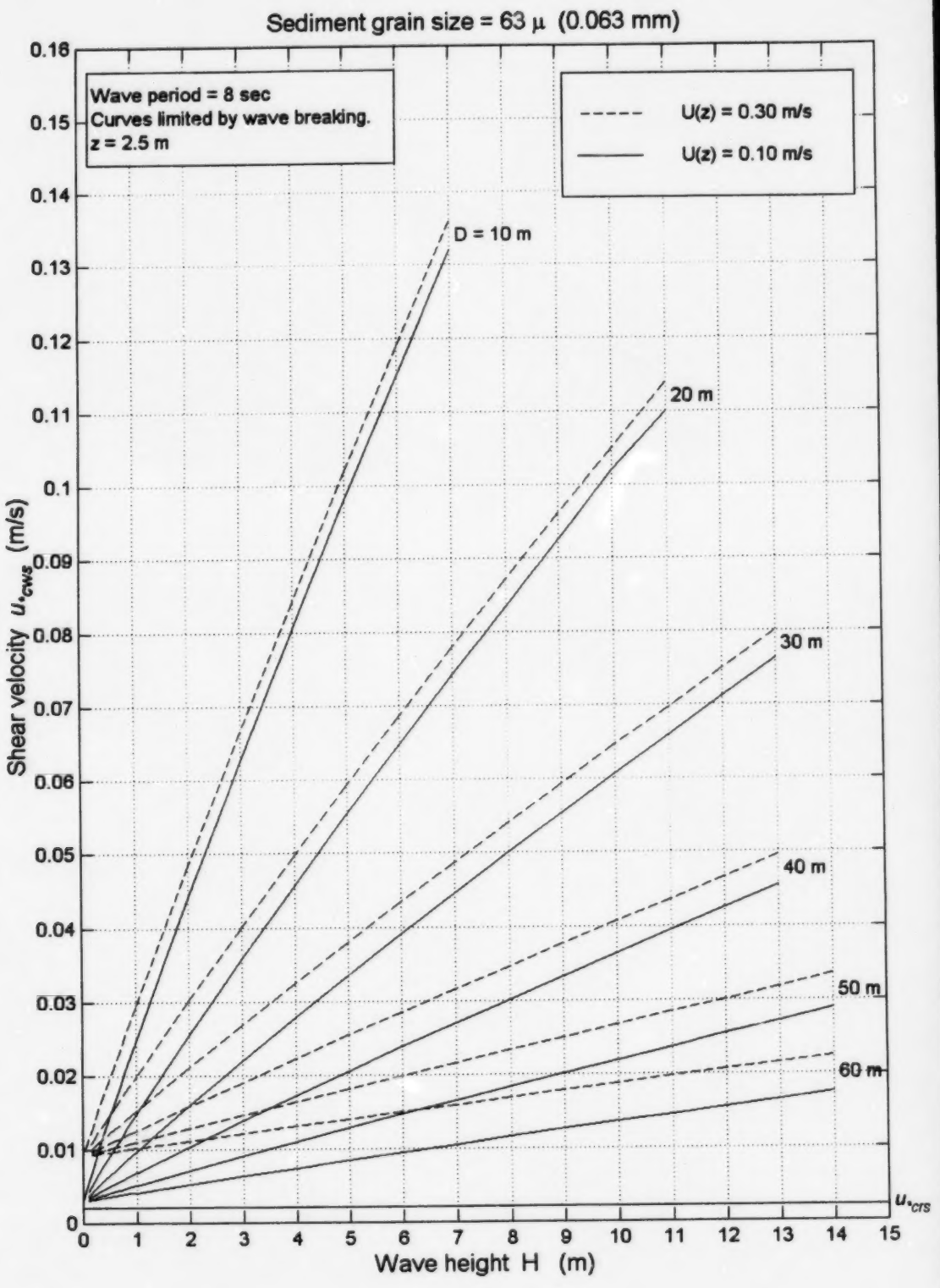

Figure 26 Seabed shear velocity u_{*cws} versus wave height for water depths from 10 to 60 m and sediment grain diameter 63μ (0. 063 mm).

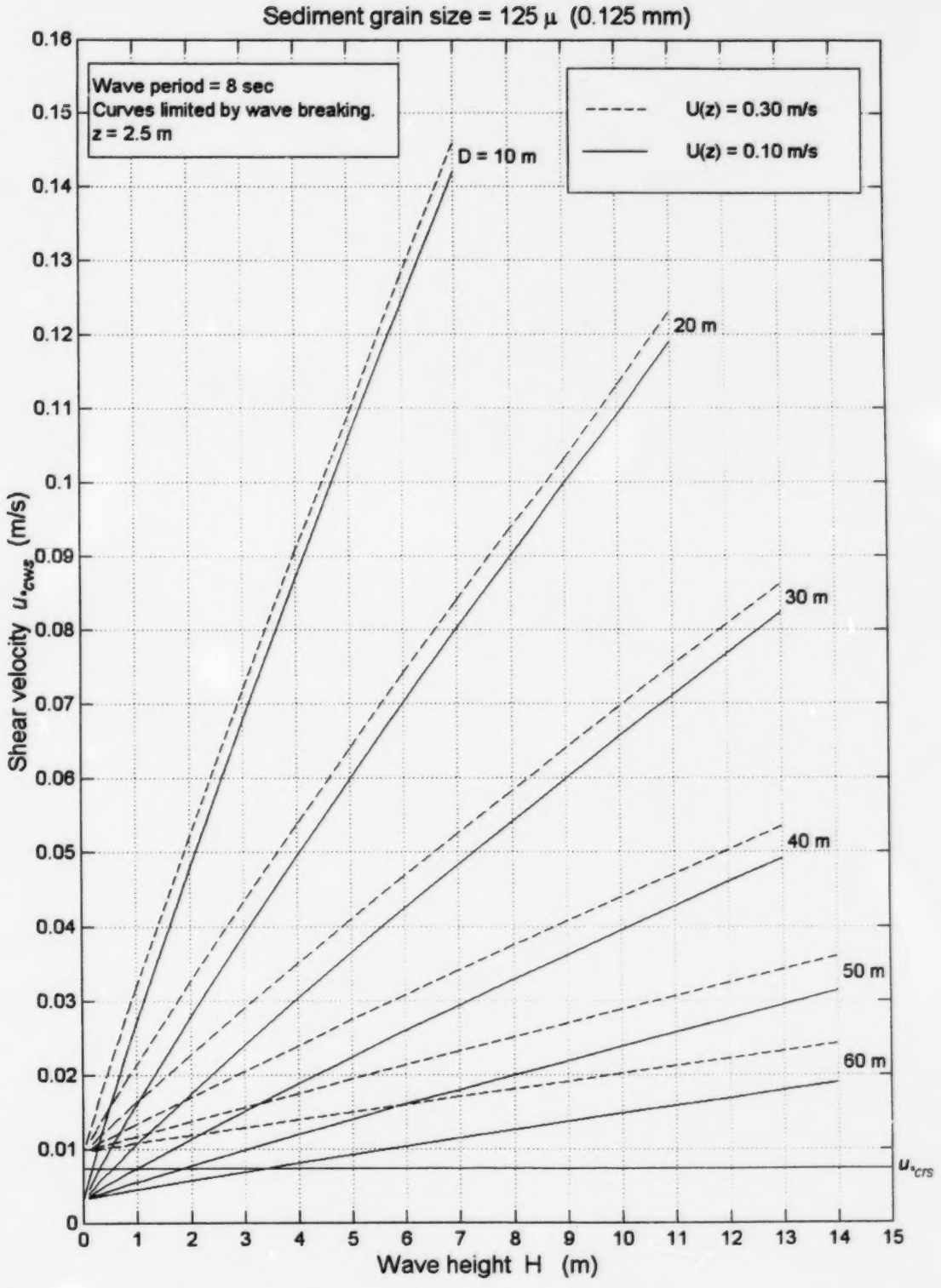

Figure 27 Seabed shear velocity u_{*cws} versus wave height for water depths from 10 to 60 m and sediment grain diameter 125μ (0. 125 mm).

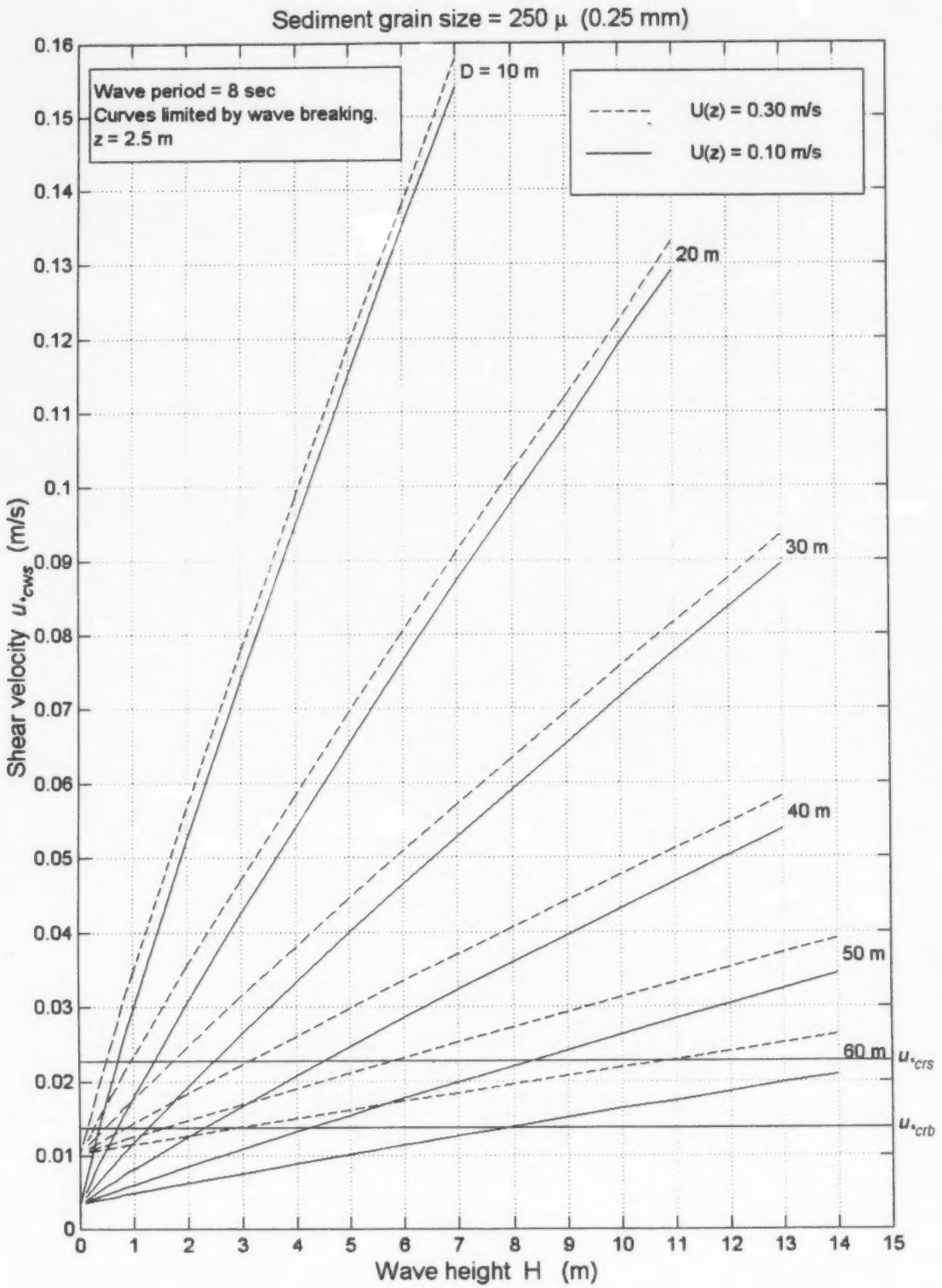

Figure 28 Seabed shear velocity u_{*cws} versus wave height for water depths from 10 to 60 m and sediment grain diameter 250μ (0. 250 mm).

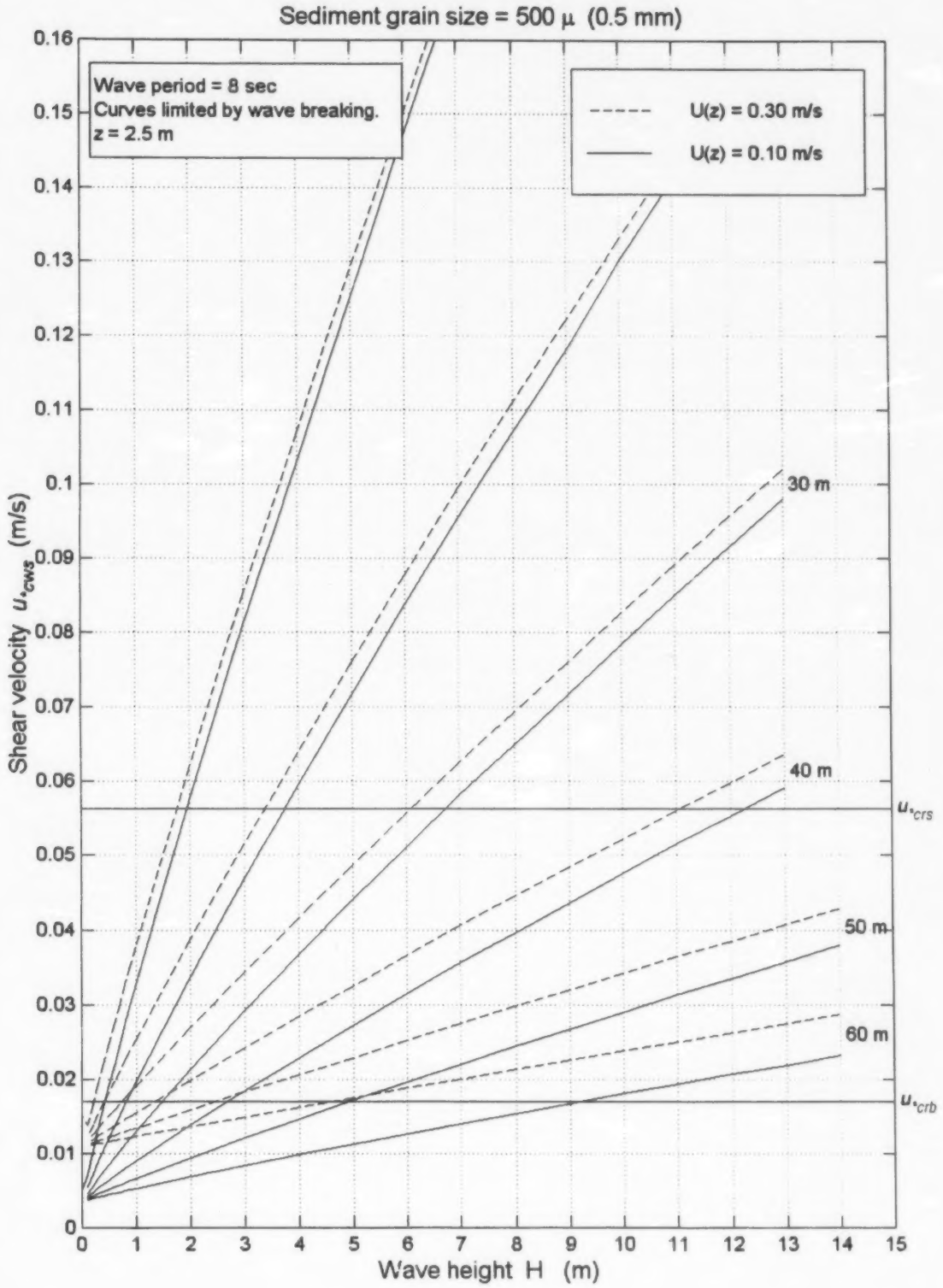

Figure 29. Seabed shear velocity u_{*cws} versus wave height for water depths from 10 to 60 m and sediment grain diameter 500μ (0. 500 mm).

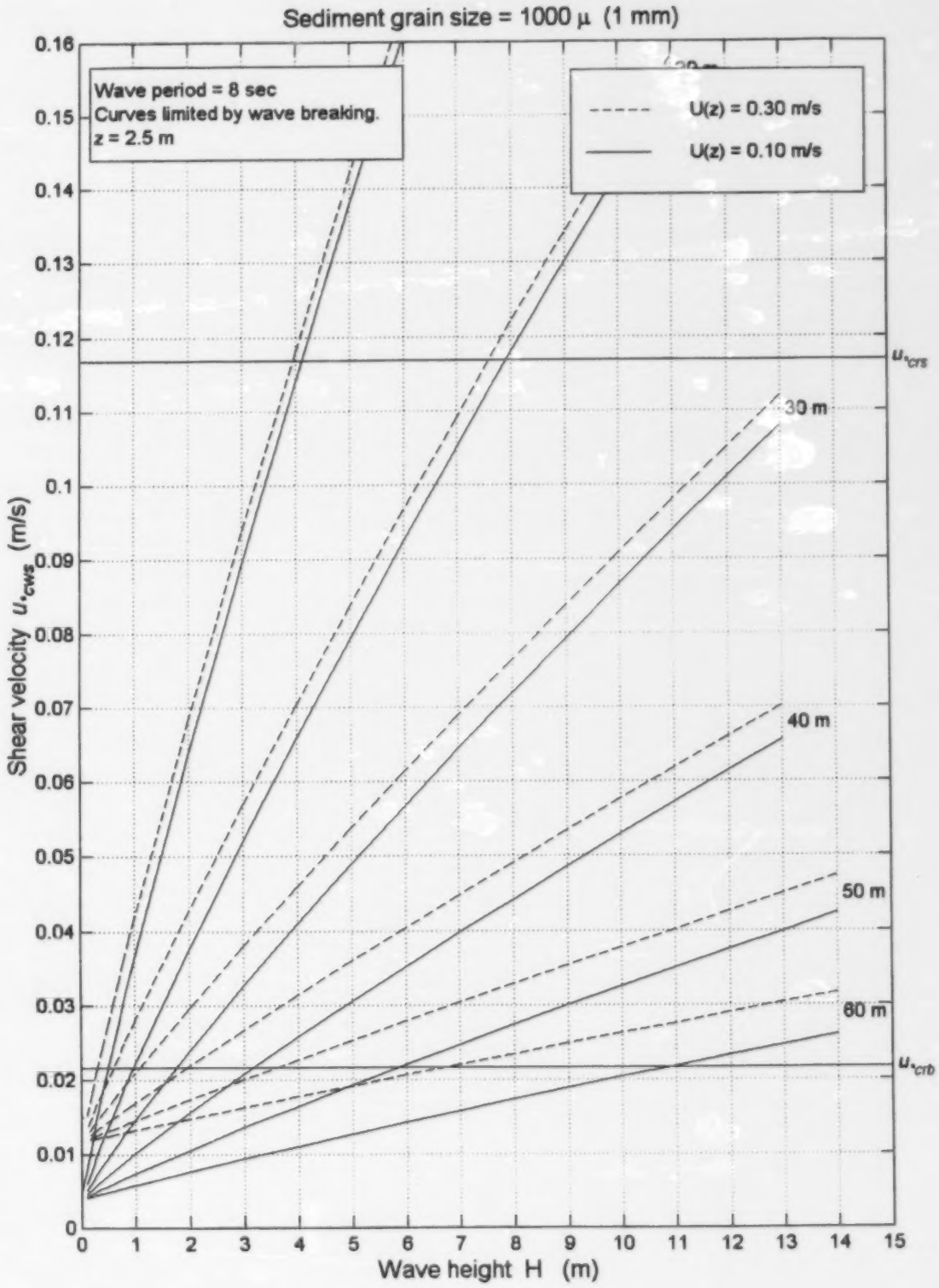

Figure 30 Seabed shear velocity u_{*cws} versus wave height for water depths from 10 to 60 m and sediment grain diameter 1000μ (0. 100 mm).

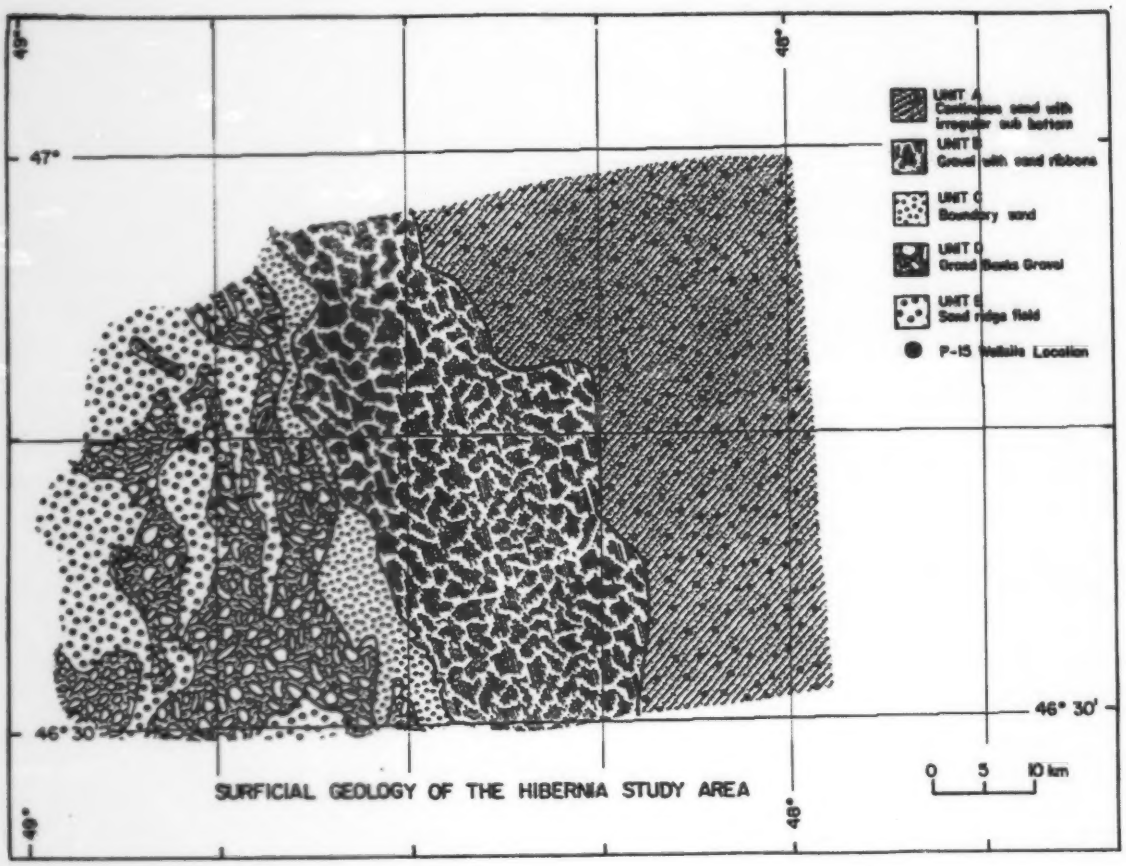

Figure 31. Surficial Geology of the Hibernia area, Northeast Grand Banks of Newfoundland. From Barrie *et al*, 1984.

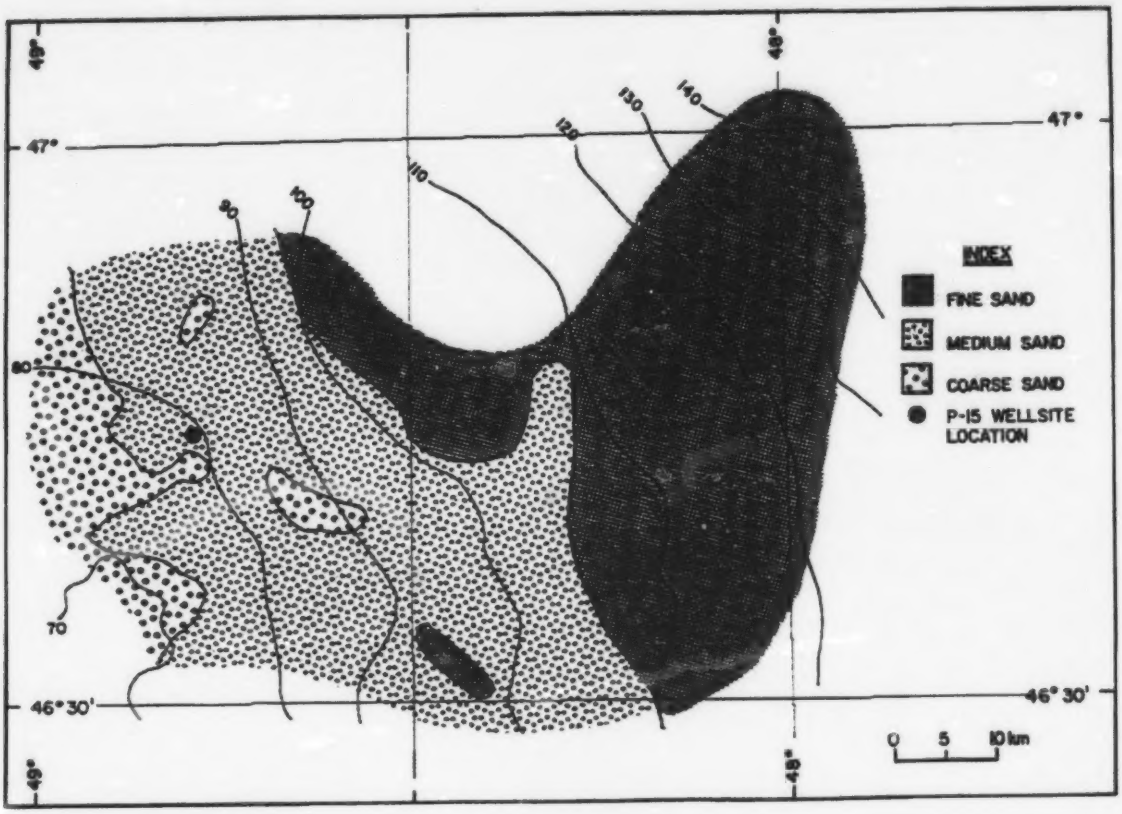

Figure 32. Surficial sediment grain size distribution, Hibernia area, Northeast Grand Banks of Newfoundland. From Barrie *et al*, 1984.

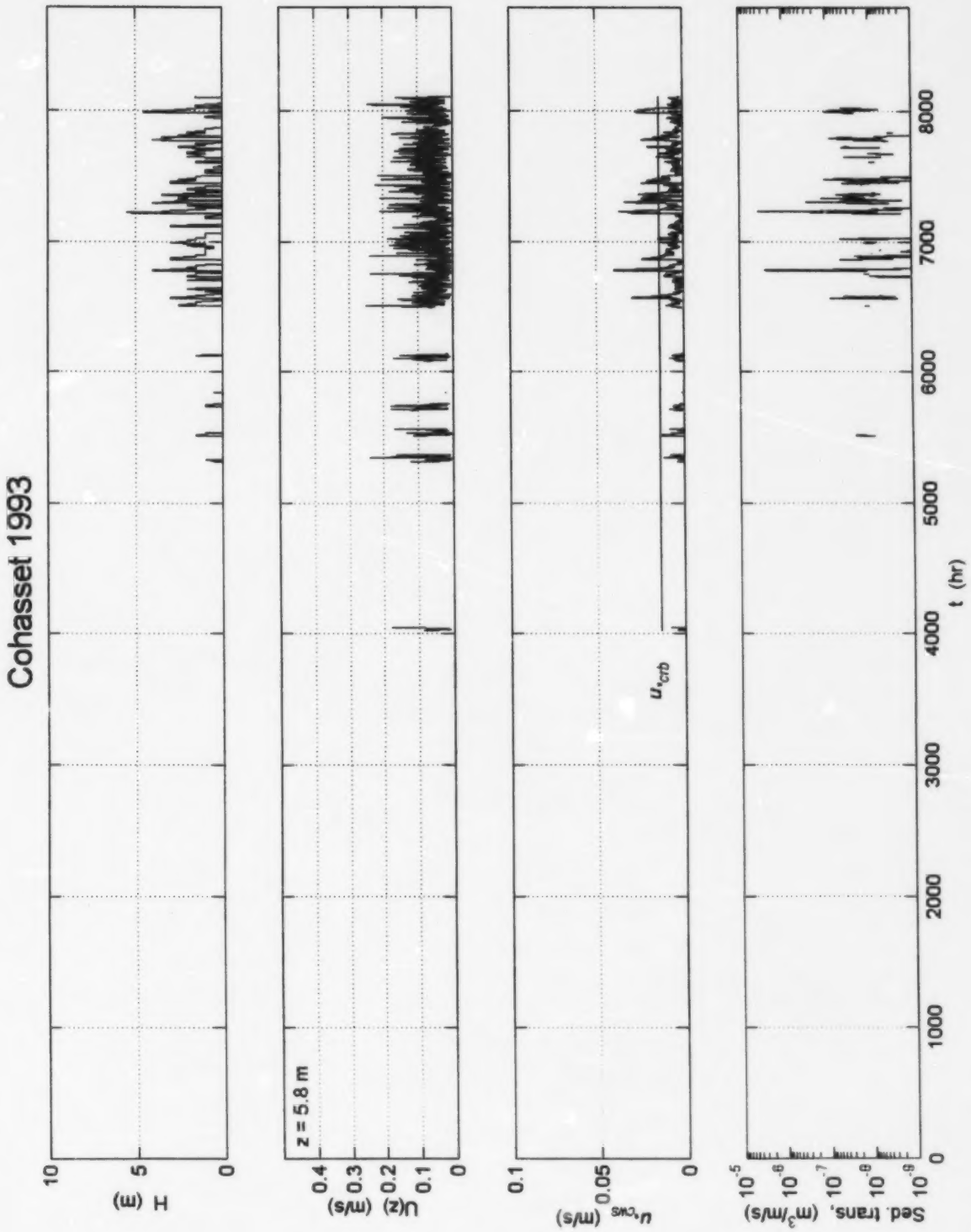

Figure 33. Hourly time series of swell height H, near-seabed current $U(z)$, skin-friction combined shear velocity u_{*cws}, and volumetric rate of sediment transport magnitude at Cohasset, 1993.

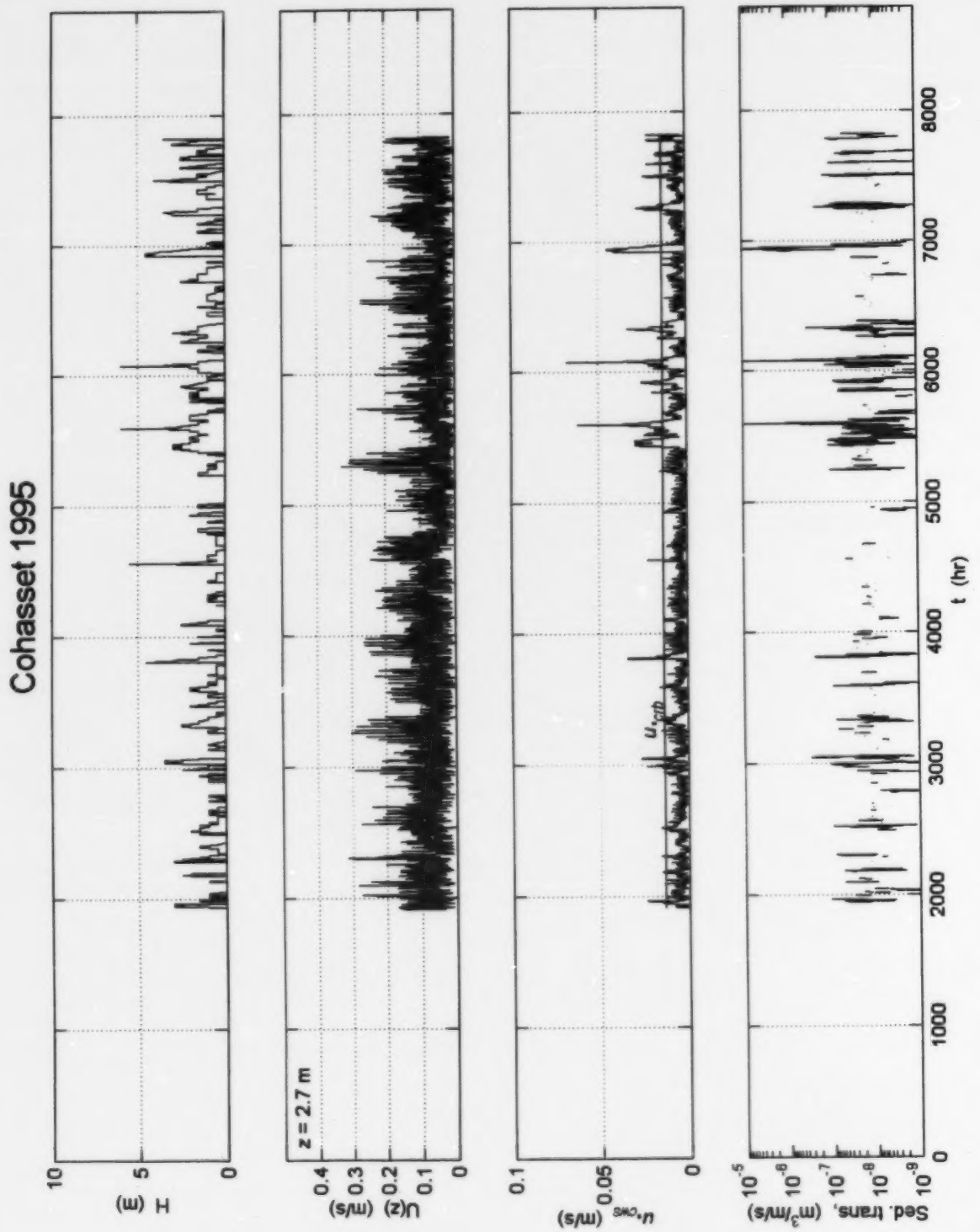

Figure 34. Hourly time series of swell height H, near-seabed current $U(z)$, skin-friction combined shear velocity u_{*cws}, and volumetric rate of sediment transport magnitude at Cohasset, 1995.

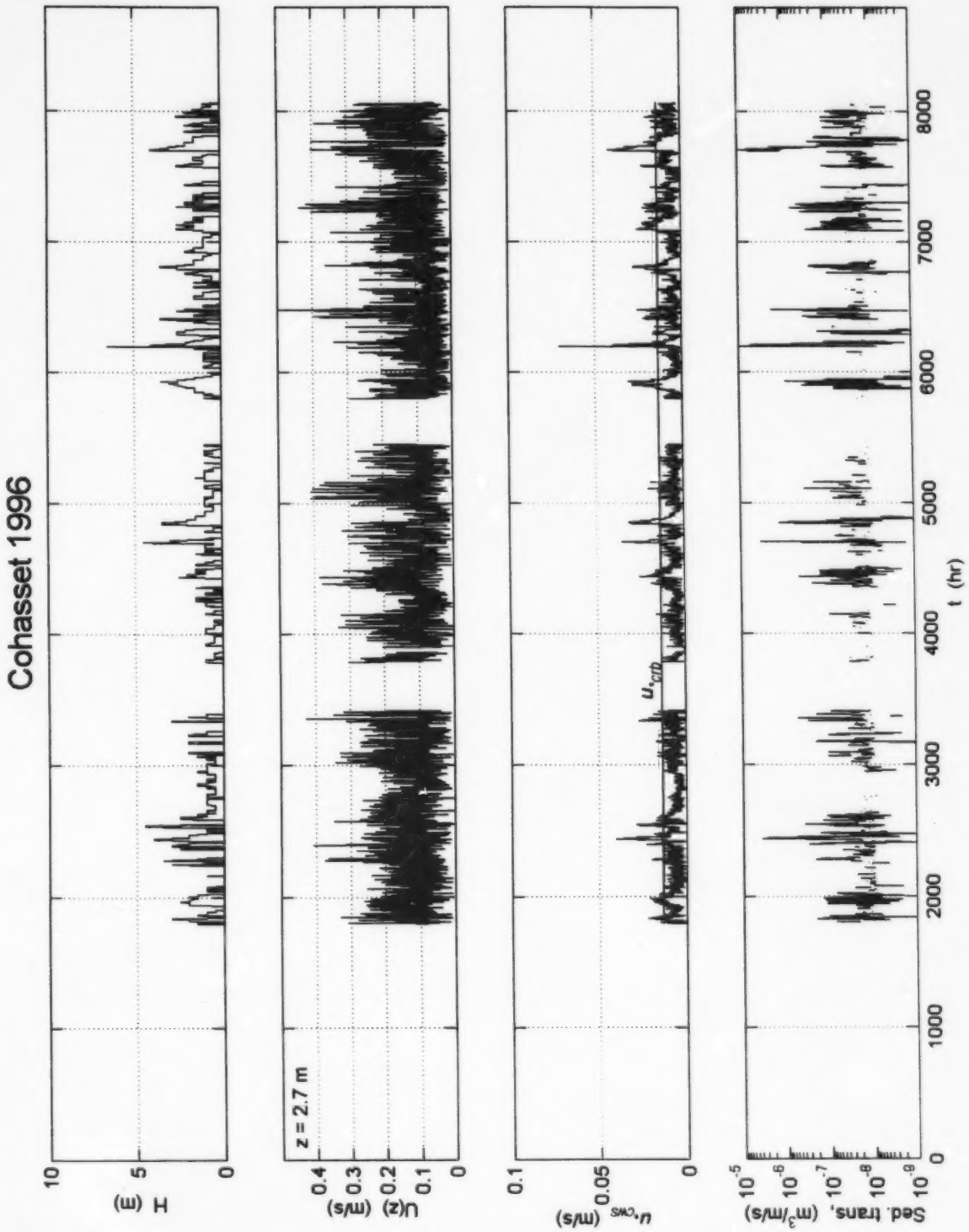

Figure 35. Hourly time series of swell height H, near-seabed current $U(z)$, skin-friction combined shear velocity u_{*cws}, and volumetric rate of sediment transport magnitude at Cohasset, 1996.

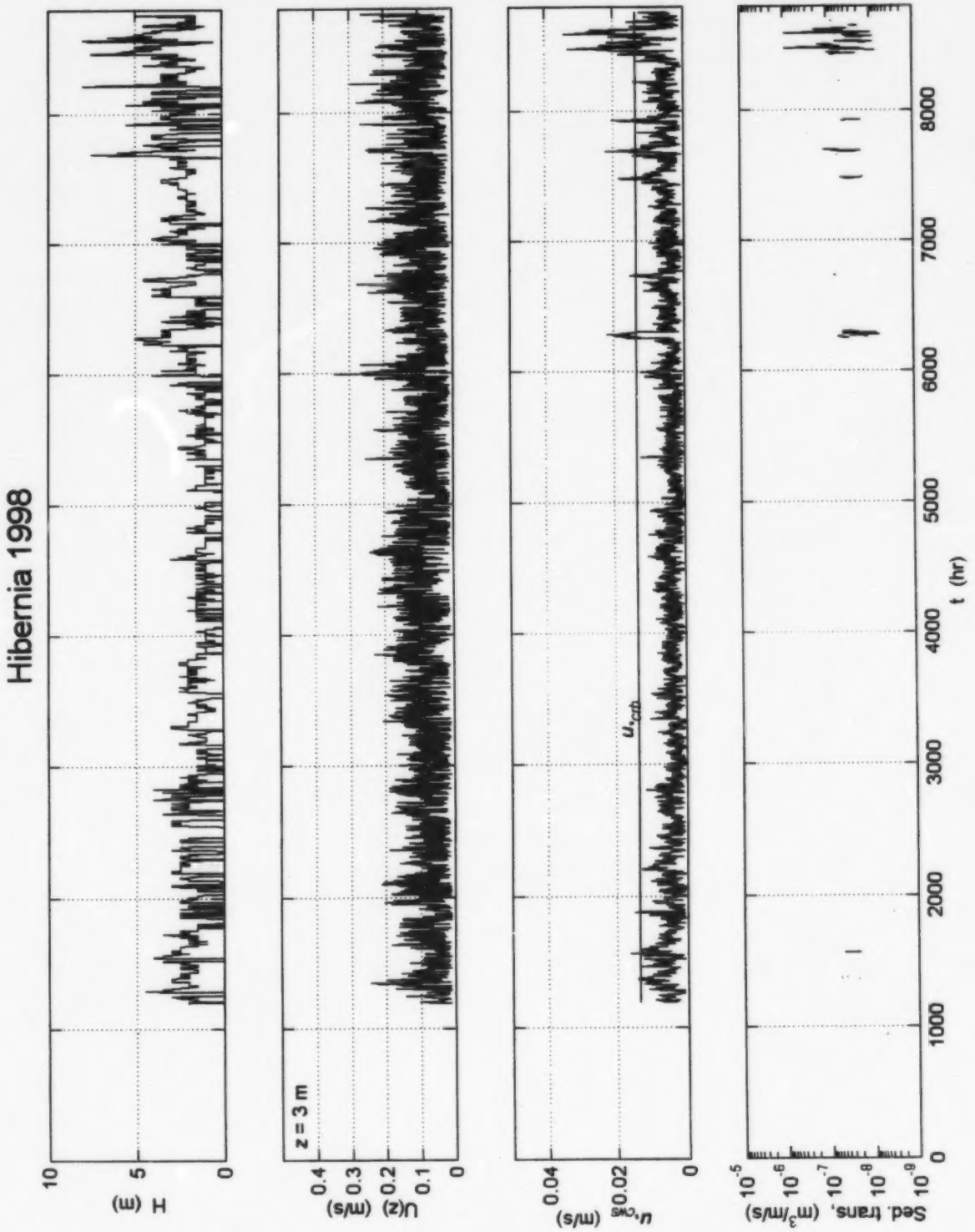

Figure 36. Hourly time series of swell height H, near-seabed current $U(z)$, skin-friction combined shear velocity u_{*cws}, and volumetric rate of sediment transport magnitude at Hibernia, 1998.

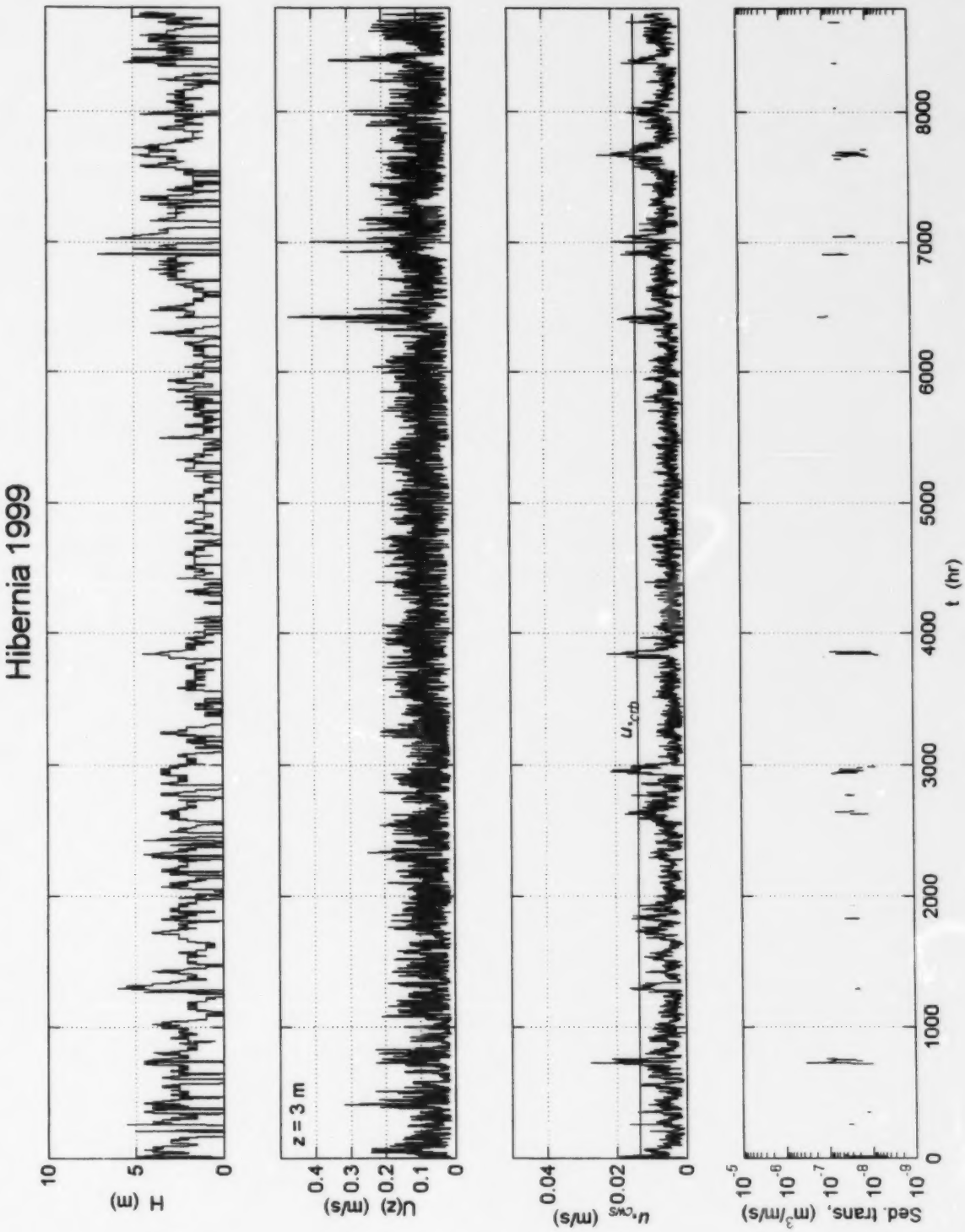

Figure 37. Hourly time series of swell height H, near-seabed current $U(z)$, skin-friction combined shear velocity u_{*cws}, and volumetric rate of sediment transport magnitude at Hibernia, 1999.

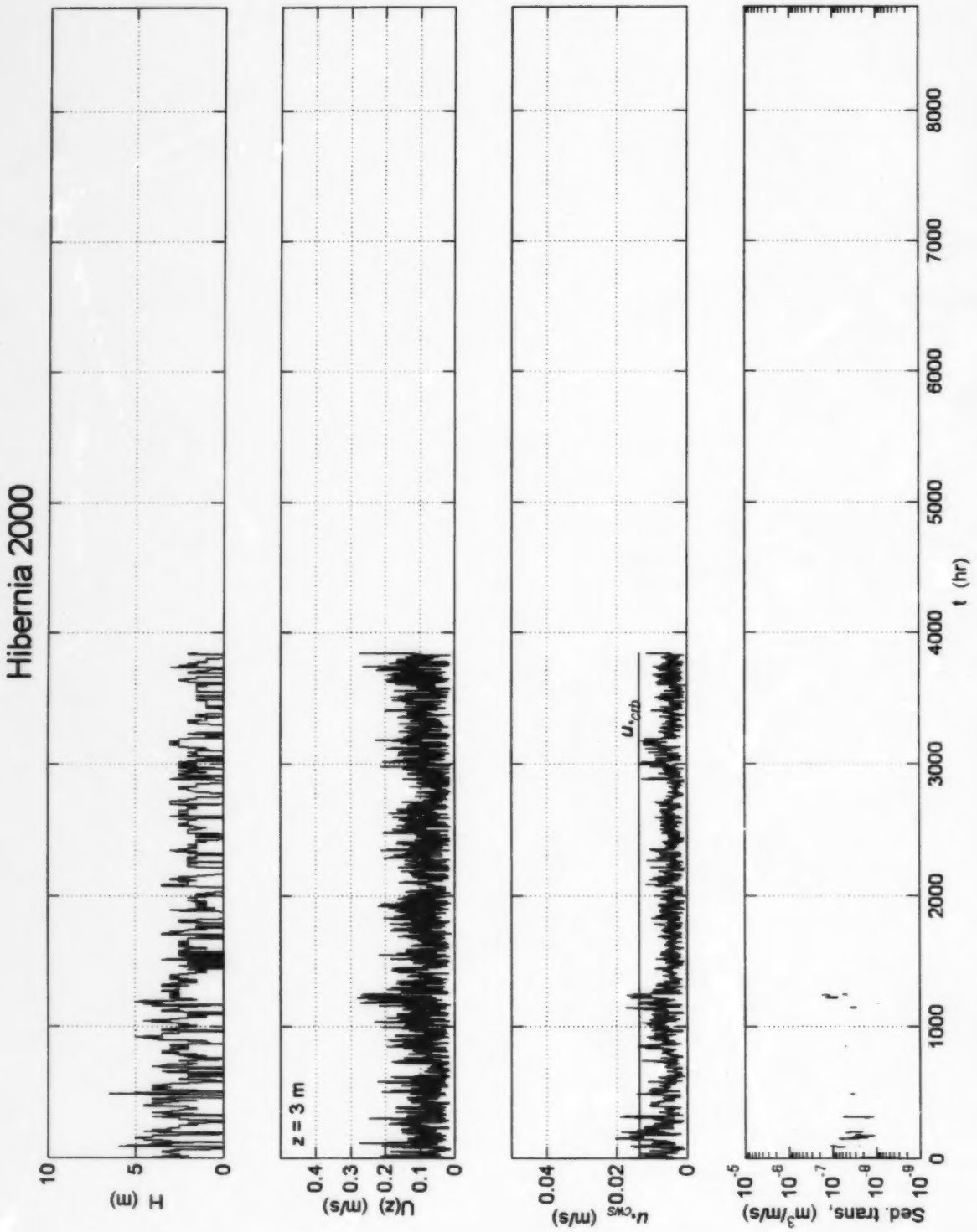

Figure 38. Hourly time series of swell height H, near-seabed current $U(z)$, skin-friction combined shear velocity u_{*cws}, and volumetric rate of sediment transport magnitude at Hibernia, 2000.